

CHALMERS



Face Lift of a Control System for Natural Gas Engines
Redesign of a Cylinder Module (CM) and a Knock Module (KM)
in a system for control of natural gas engines.

Master of Science Thesis in the Programme IESD

Ulrika Ahlquist

Department of Computer Science and Engineering
CHALMERS UNIVERSITY OF TECHNOLOGY
UNIVERSITY OF GOTHENBURG
Göteborg, Sweden, June 2009

The Author grants to Chalmers University of Technology and University of Gothenburg the non-exclusive right to publish the Work electronically and in a non-commercial purpose make it accessible on the Internet.

The Author warrants that he/she is the author to the Work, and warrants that the Work does not contain text, pictures or other material that violates copyright law.

The Author shall, when transferring the rights of the Work to a third party (for example a publisher or a company), acknowledge the third party about this agreement. If the Author has signed a copyright agreement with a third party regarding the Work, the Author warrants hereby that he/she has obtained any necessary permission from this third party to let Chalmers University of Technology and University of Gothenburg store the Work electronically and make it accessible on the Internet.

Face Lift of a Control System for Natural Gas Engines
Redesign of the Cylinder Module (CM) and the Knock Module (KM) in a system for control of natural gas engines.

Ulrika Ahlquist

© Ulrika Ahlquist June 2009.

Examiner: Lars Svensson

Department of Computer Science and Engineering
Chalmers University of Technology
SE-412 96 Göteborg
Sweden
Telephone + 46 (0)31-772 1000

Cover picture:

Control and Modules (CM – bottom left, KM – bottom right and MC – top right) and ignition unit (top right) for a natural gas engine, see detailed information on page 1.

Department of Computer Science and Engineering
Göteborg, Sweden June 2009

Abstract

The purpose of this project is to guarantee spare parts of an EMS (Engine Management System for Natural Gas) electronic engine control system for natural gas engines for as long as they may be needed. This is done by redesigning the old system using state of the art components. The redesign will also improve the mechanical reliability of the system. The EMS system is used in several large stationary engines, all being available in several different versions. EMS is used in engines with up to 18 cylinders. This project covers the hardware only, no work has been done on the software.

The project is carried out at Hoerbiger Control Systems AB in Åmål and the work follows the V-model for project development. The components in the design have been analyzed so that for the components no specified limits are exceeded and that the functional requirements of the system are satisfied. The redesign of the system resulted in increased mechanical reliability but the functionality of the system cannot be verified until the software has been developed.

Syftet med detta projekt är att säkerställa reservdelar för EMS (Engine Management System for Natural Gas) motorstysystemet så länge som de behövs. Detta görs genom en omkonstruktion av dagens system med nyare och modernare komponenter. Omkonstruktionen kommer också att öka den mekaniska tillförlitligheten. EMS används i ett flertal stora stationära motorer som alla finns i flera olika varianter. EMS används på motorer upp till 20 cylindrar. Detta projekt omfattar endast hårdvaran, inget arbete har gjorts på mjukvaran.

Projektet har gjorts åt Hoerbiger Control Systems AB i Åmål och arbetet har följt V-modellen för projektutveckling. Beräkningar på komponenterna som använts i konstruktionen har utförts så att de belastas i det för komponenten specificerade området och att kravspecifikationen för systemet uppfylls. Omkonstruktionen av systemet resulterade i en ökad mekanisk tillförlitlighet men systemets funktioner kan inte verifieras förrän mjukvaran utvecklats.

Preface

This report is the result of my master thesis work at the study programme for Integrated Electronic Systems Design (IESD) at Chalmers University of Technology, Göteborg. The project was done at Hoerbiger Control Systems AB in Åmål and at the Department of Computer Science and Engineering at Chalmers. Mikael Grufman was my supervisor at Hoerbiger and Lars Svensson was my examiner at Chalmers.

I would especially like to thank Mikael for his advice and support. I also would like to thank everyone else at Hoerbiger for helping me in my work.

I give a special thank you to my darling Styrbjörn for believing in me and supporting me during my 5 years of studies at the university.

Åmål, June 2009.

Ulrika Ahlquist

Table of contents

1	INTRODUCTION	1
1.1	Background	1
1.2	Limitations	2
1.3	Hoerbiger Control Systems AB	2
2	NATURAL GAS ENGINE	2
2.1	Industrial Natural Gas Engine	2
2.2	Engine Control System	3
3	METHOD	5
3.1	The V-model	5
4	ANALYSES	6
4.1	Main Functionality of the CM and KM	6
4.2	MPC5632M and MPC5534 Microcontroller	8
4.2.1	1.2 V Power Supply for the Microcontroller	9
4.2.2	Crystal Oscillator	11
4.2.3	Programming the Microcontroller	11
4.2.4	Input and Output Signals	11
4.3	Main CC and PCC Injectors - CM	12
4.3.1	Freewheeling and Clamping	13
4.3.2	Power Loss in the Injector Drive Transistor	19
4.3.3	Power Loss in the Freewheeling Diode	21
4.3.4	Current Sensing	22
4.3.5	Protection from Short Circuit Connection	23
4.4	Ignition Timing - CM	27
4.5	CAN - CM and KM	27
4.6	Thermocouples - CM	28
4.7	Engine Position Signals - CM and KM	29
4.8	Knock - KM	36
4.9	Power Supply	37
4.10	Printed Circuit Board	40
4.10.1	Design Rules	40
4.10.2	PCB Design	41
4.11	Reliability Prediction of Electronic Equipment	42
5	RESULT	44
6	DISCUSSION	45
7	TERMINOLOGY	46
8	REFERENCES	47

Appendix 1 – Cylinder Module PCB

Appendix 2 – Knock Module PCB

Appendix 3 – Customer Requirements Document

List of Figures

- Figure 1-1: The EMS system 1
- Figure 2-1: The Wärtsilä 34SG engine. By courtesy of Wärtsilä [2] [3] [4] 2
- Figure 2-2: Bloch schematic of the EMS engine control system with external units 3
- Figure 2-3: Block diagram with the connection of the CM to other units on the engine..... 4
- Figure 2-4: Block diagram with the connection of the KM to other units on the engine 4
- Figure 3-1: The Development model for Hoerbiger Control Systems..... 5
- Figure 4-1: Block schematic of the CM with external units 7
- Figure 4-2: Block schematic of the KM with external units 7
- Figure 4-3: MPC5632M block diagram [6] 9
- Figure 4-4: Schematic with internal regulator to provide 1.2 V (VDD) for the core..... 9
- Figure 4-5: Rotary switch used to identify the CM..... 11
- Figure 4-6: Injector current and time definitions 12
- Figure 4-7: Simplified schematic of freewheeling and clamping methods..... 13
- Figure 4-8: Current through the transistor when a freewheeling diode is used 14
- Figure 4-9: Current through the freewheeling diode..... 14
- Figure 4-10: Simulation in OrCAD of a clamping circuit 15
- Figure 4-11: Simulation in OrCAD with a freewheeling circuit..... 16
- Figure 4-12: Inductor current simulation in OrCAD 17
- Figure 4-13: Simplified schematic of HSD and LSD with the clamping method to the left and the freewheeling method to the right..... 18
- Figure 4-14: Injector current control with the clamping and freewheeling methods..... 18
- Figure 4-15: Current sensing..... 22
- Figure 4-16: Protection from short circuit connection using a thyristor 23
- Figure 4-17: Injector driver using freewheeling diodes protected from short circuit connection 26
- Figure 4-18: Injector driver using the clamping method protected from short circuit connection 26
- Figure 4-19: Schematic of the spark delivery activation..... 27
- Figure 4-20: Schematic of the CAN interface..... 27
- Figure 4-21: Schematic of the indication with a LED of correct operation of the CAN communication 27
- Figure 4-22: Schematic of thermocouple inputs using MAX6675ISA..... 28
- Figure 4-23: Schematic of thermocouple inputs using AD595 28
- Figure 4-24: Wärtsilä 34SG engine. By courtesy of Wärtsilä [29][4] 29
- Figure 4-25: Differential amplifier as a current sensor 30

Figure 4-26: Schmitt trigger with variable hysteresis	31
Figure 4-27: Schmitt trigger hysteresis	31
Figure 4-28: Schematic of the KM engine position signals	32
Figure 4-29: Boost of the crank and cam signals in the KM to the CM and the effect of the protection from short circuit connection	33
Figure 4-30: Simulation of the protection from short circuit connection of the engine position circuit.....	34
Figure 4-31: Schematic of the CM engine position signals (crank and cam signals)	34
Figure 4-32: Definition of time response for PC357.....	35
Figure 4-33: Definitions of V_{T+} , V_{T-} and V_H	36
Figure 4-34: Differential amplifier for the knock signal.....	37
Figure 4-35: CM power supply schematic	38
Figure 4-36: KM power supply schematic	39
Figure 4-37: Schematic of the indication with a LED of correct power supply to the microcontroller	40

List of Tables

Table 4.1: Specification for the transistor BCP68T1	10
Table 4.2: Measured inductance and resistance for the injector valves	13
Table 4.3: Power and temperature calculations for the injector driver using freewheeling diode for different engines	20
Table 4.4: Power and temperature calculations for the injector driver using the clamping method for different engines	21
Table 4.5: Power and temperature calculations for the freewheeling diode for different engines.....	22
Table 4.6: Maximum and minimum component values from datasheets	24
Table 4.7: Protection from short circuit connection using a thyristor.....	24
Table 7.1: Terminology.....	46

1 Introduction

1.1 Background

EMS (Engine Management System for Natural Gas) is an electronic engine control system for natural gas engines. It was designed in the early 90s by Mecel AB in Åmål and there are over 600 engines world-wide equipped with EMS in use today. The majority of these engines will be in operation beyond 2020. The purpose of this work is to guarantee spare parts for the EMS for as long as they may be needed. This is done by redesigning the current system with state of the art components. The redesign may also increase the mechanical reliability of the system and possibly also reduce the cost.

The EMS system consists of four different parts: the Cylinder Module (CM), Knock Module (KM), Master Controller (MC) and the Ignition Unit (IU), see Figure 1-1. There is one CM for every two cylinders, one KM for every nine cylinders, one MC for each engine and one ignition unit for every cylinder.



Figure 1-1: The EMS system. Top left – IU, top right – MC, bottom left – CM and bottom right – KM

This project is focused on the redesign of the CM and the KM hardware. The MC is not a part of this project and the ignition unit does not need to be redesigned since it consists of common components that will be available for a very long time. The current CM and KM consist of two printed circuit boards (PCB) each, one I/O-board and one CPU board. One of the purposes of this project is to remove one PCB in each unit.

1.2 Limitations

This project only redesigns the hardware and not the software. The work on the software will be done at a later time. It is therefore not possible to build a prototype and test the design.

A further requirement is that the mechanical design of the casing and functionality of the system must not be changed. The PCB must therefore be mounted in the same position in the casings as one of the PCBs used in the current system.

1.3 Hoerbiger Control Systems AB

Hoerbiger Control Systems AB was founded in Åmål in 1982 as Mecel AB. The business idea was to develop and sell advanced development projects in the field of engine control to the automotive industry. In 2007 Mecel in Åmål joined the Hoerbiger Group and the company name was changed to Hoerbiger Control Systems AB. The focus today is on industrial engines and only a small part of the company still works with the automotive engines. Hoerbiger Control Systems AB has 31 employees in Åmål; the Hoerbiger Group has about 6400 employees worldwide in over 90 countries and a net sale of almost 1000 million Euros.

2 Natural Gas Engine

Most natural gas engines today are large stationary engines. Although there are some car engines that can be run on natural gas and petrol, those are called bi-fuel systems. The gas consists mostly of methane (CH_4). The methane is cleaned and then compressed to form Compressed Natural Gas (CNG). The cylinder pressure is higher in a natural gas engine than in a petrol engine.

2.1 Industrial Natural Gas Engine

The EMS is an electronic engine control system for industrial natural gas engines. Cummins, MAN and Wärtsilä are examples of manufacturers of such engines. The Wärtsilä 34SG engine [1] is one example of a large industrial natural gas engine, see Figure 2-1. Most natural gas engines are spark-ignited engines that work according to the Otto process and the lean-burn principle. The Otto engine was developed by Nikolaus Otto (1832 - 91). It is a four stroke internal combustion engine with spark plugs. Engines with lean burn can employ higher compression ratios and thus provide better performance, more efficient fuel use and lower hydrocarbon emissions.



Figure 2-1: The Wärtsilä 34SG engine. By courtesy of Wärtsilä [2] [3] [4]

2.2 Engine Control System

Figure 2-2 shows a block schematic of the EMS system. A photo of the four parts marked with blue borders is shown in Figure 1-1.

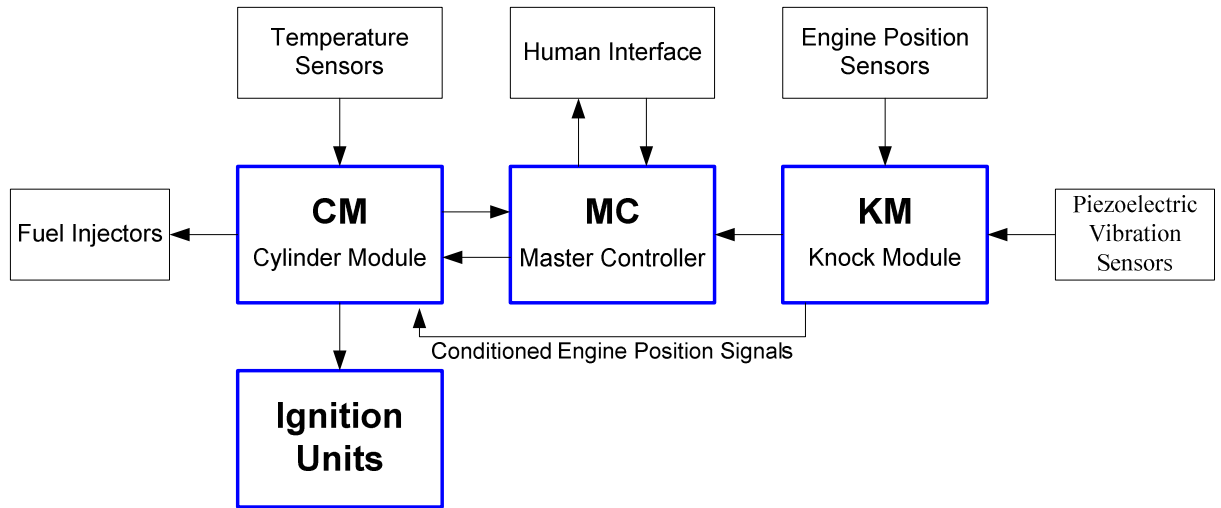


Figure 2-2: Block schematic of the EMS engine control system with external units

The engine performance can be optimized by controlling the following main functions of the engine:

- Fuel gas feed to the engine
- Charge air flow to the engine
- Cylinder individual fuel gas flow control
- Cylinder individual ignition control

The MC, see Figure 1-1, processes all engine information received from the other engine units and transmits all data to the CM and KM for necessary optimal engine performance. The CM, see Figure 1-1 and Figure 2-3, controls the fuel injection and ignition for two cylinders on the engine. Figure 2-3 shows a block diagram of the CM and the connections to other units on the engine. The CM has actuator outputs for injection and ignition control and inputs for K-type TC temperature sensors and for crank and cam engine position signals. It also has a CAN bus interface for data communication between the different units in the system. The MC sends fueling and ignition data on the CAN bus to the CM. The CM also receives crank and cam signals from the engine position sensors and from those signals decides when to activate fuel injection and spark delivery.

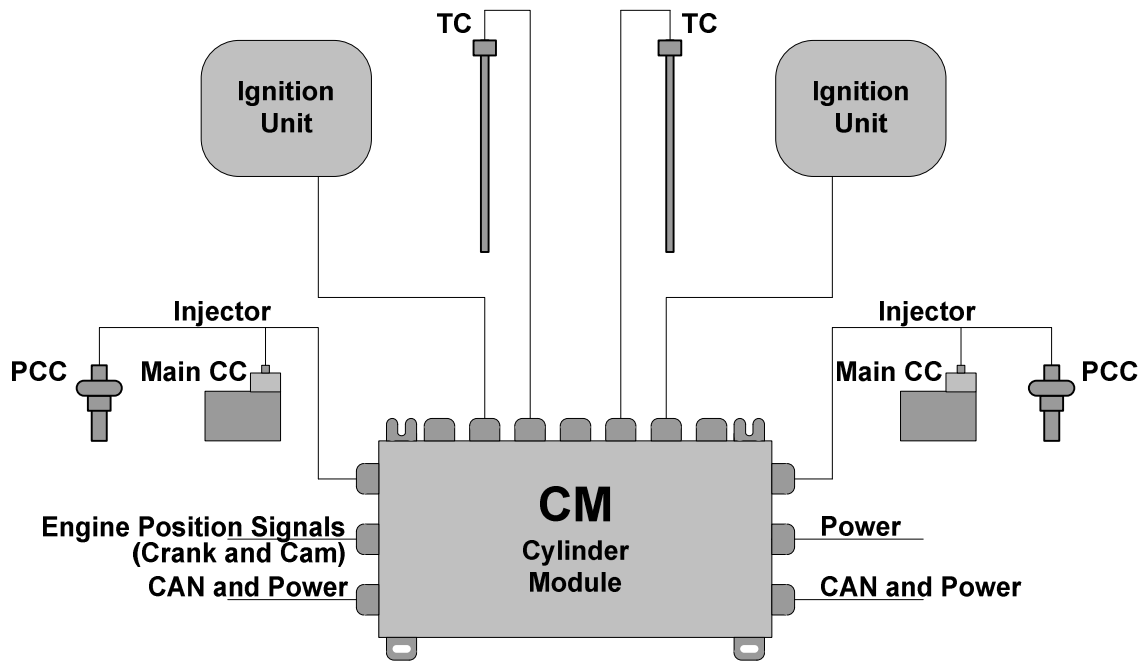


Figure 2-3: Block diagram with the connection of the CM to other units on the engine

The KM, see Figure 1-1 and Figure 2-4, detects knock. Knock is an uncontrolled simultaneous self-ignition after ignition of the fuel that will lead to a sudden increase of the pressure resulting in damage to the engine. The KM receives inputs from vibration sensors on each cylinder, processes the signals and then sends the information over the CAN bus to the MC.

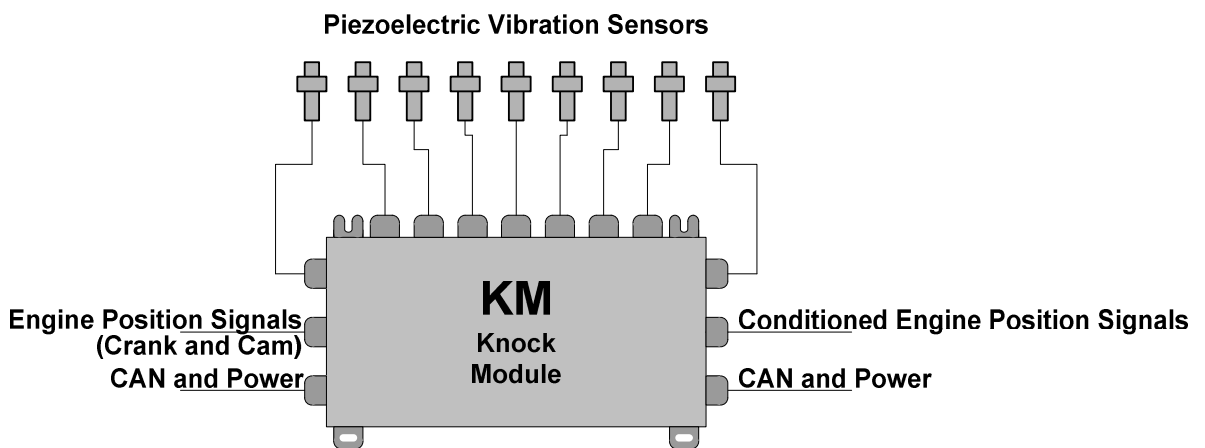


Figure 2-4: Block diagram with the connection of the KM to other units on the engine

The ignition unit, see Figure 1-1, generates the high voltage that creates the spark in the spark plug to ignite the fuel. The ignition unit is controlled by the CM.

3 Method

The project work follows the Hoerbiger Control Systems AB's (HCO) development model in their Quality Handbook (QHB), described in 3.1. The master thesis will therefore be carried out in the same way as any other development project at Hoerbiger Control Systems AB.

3.1 The V-model

The project will follow the V-model, see Figure 3-1. The V-model begins with a quote and then a Customer Requirement Document (CRD).

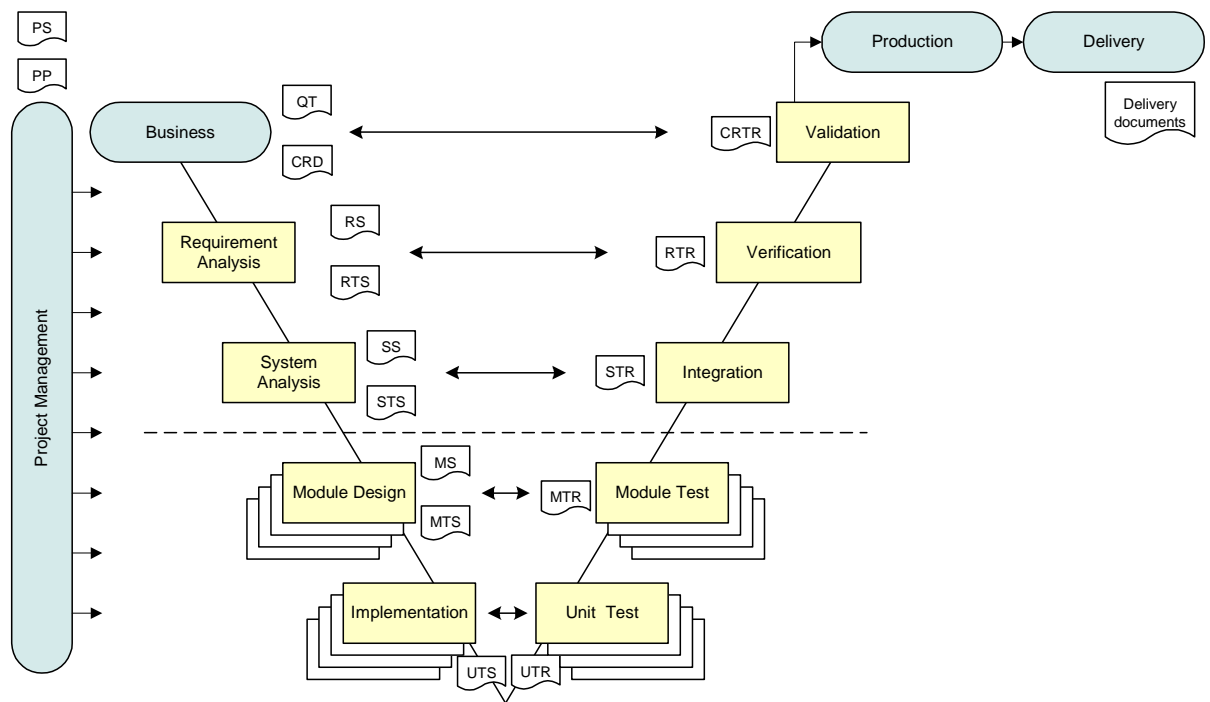


Figure 3-1: The Development model for Hoerbiger Control Systems

The CRD is broken down in smaller and more detailed internal requirements: first to a Requirement Specification (RS), then to a System Specification (SS) and finally to a Module Specification (MS). Each document is reviewed and approved before the next step begins. The MS is the basis for the hardware design.

4 Analyses

EMS is used for different engines. The same PCB is used for all engines and it must therefore be designed according to the toughest requirements in all engine specifications. Doing a facelift on a 15 year old design is almost like changing the entire design. The reason for this is of course the rapid development of new components, especially microcontrollers but also of new power semiconductors and other integrated circuits.

4.1 Main Functionality of the CM and KM

The main functionality of the CM is to

- Control two main gas and two Pre-Combustion Chamber (PCC) gas injectors
- Control the ignition timing with an ignition control signal to the ignition units
- Communicate via a CAN link with a baud rate of 0.5 Mbit
- Measure four exhaust temperatures, two for each cylinder with K-type thermocouples (TC)
- Decode the crank and cam signals transmitted from the KM to detect engine position and phasing

The main functionality of the KM is to

- Detect knock in the cylinders through the piezoelectric vibration sensors inputs
- Transfer knock information via the CAN bus to the MC
- Decode signals from the crankshaft position sensor and the camshaft position sensor to detect engine position and phasing, crank and cam signals
- Amplify the crank and cam signals from the sensors and transmit them to the CM

Summary of the main specification:

- 19 – 29 V input voltage
- Reverse battery protection, - 29 V.
- -40°C to +85°C ambient temperature
- 0 – 1800 rpm

Figure 4-1 and Figure 4-2 show the hardware blocks in the CM, the KM and the external units that are connected to them.

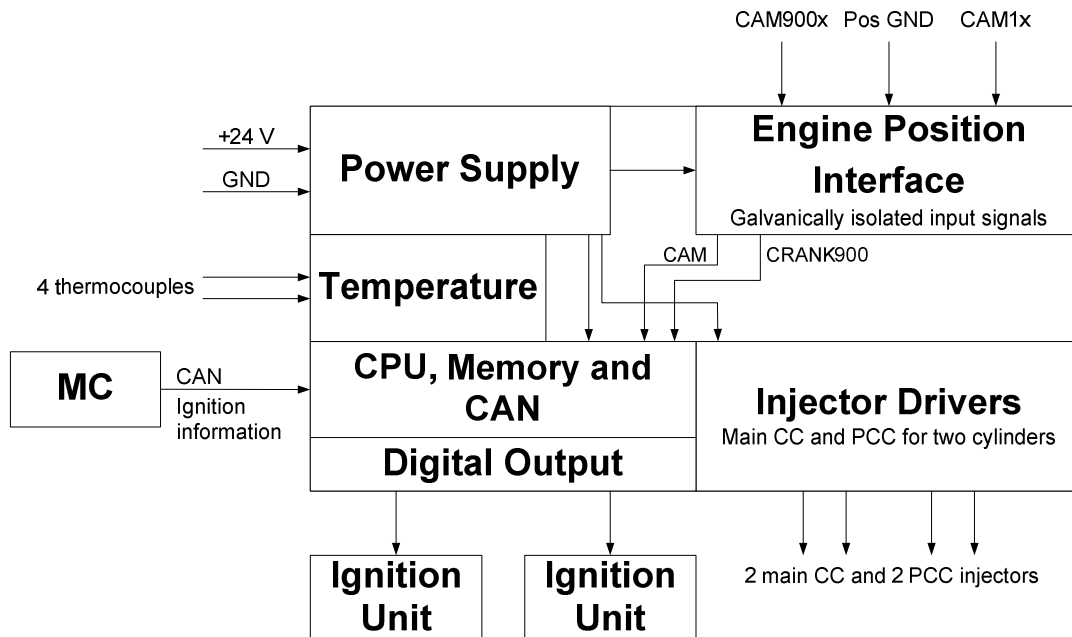


Figure 4-1: Block schematic of the CM with external units

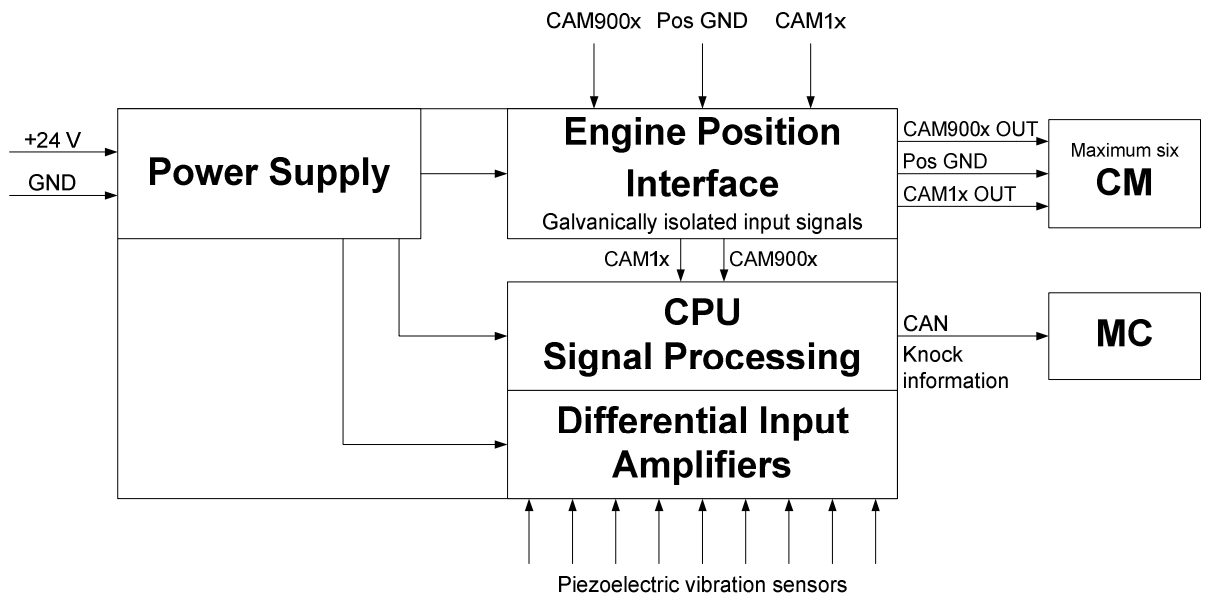


Figure 4-2: Block schematic of the KM with external units

4.2 MPC5632M and MPC5534 Microcontroller

Today there are reasonably priced microprocessors available that are much more powerful than the 15 years old microcontroller that is used in the current EMS. The development of microcontrollers has roughly followed Moore's Law [5] since the first microcontroller was developed in the 70s. The memory for instance is much larger in a microcontroller today than it was 15 years ago. By using a modern microcontroller much of the functions implemented in hardware in the current EMS system can be replaced by software.

There are several very powerful microcontrollers designed for different types of applications. The MPC5632M [6] [7] and MPC5534 [8] microcontrollers are two examples. They have integrated technologies, such as an enhanced time processor unit (eTPU), enhanced queued analog-to-digital converter (eQADC), Controller Area Network (CAN), and an enhanced modular input-output system (eMIOS), see Figure 4-3.

MPC5632M/MPC5633M

- CPU e200z3
- 768kB/1MB Flash. 32kB/64kB RAM
- TPU2, DMA, DSP, 2 x CAN, 2 x SPI, 2 x SCI
- 12 bit A/D with IIR and FIR filter
- 5V only supply
- 100/144 LQFP, 208 PBGA
- Produced by Freescale and ST
- PPC5633MMLQ80 and PPC5633MMM80 – active

MPC5534

- CPU e200z3
- 1 MB Flash, 64 kB RAM
- TPU2, DMA, SCI x 2, SPI x 2, CAN x 2
- 12 bit A/D
- Supply 3.3V and 5V
- 324 PBGA
- In production

The new MPC5632M [6] [7] microcontroller from Freescale Semiconductor is used in the EMS facelift. The main reasons for using MPC5632M instead of for instance MPC5534 is that it has 5 V single power supply with internal regulators to provide 3.3 V and 1.2 V for the core, 12 bit A/D with IIR and FIR filter and a LQFP package.

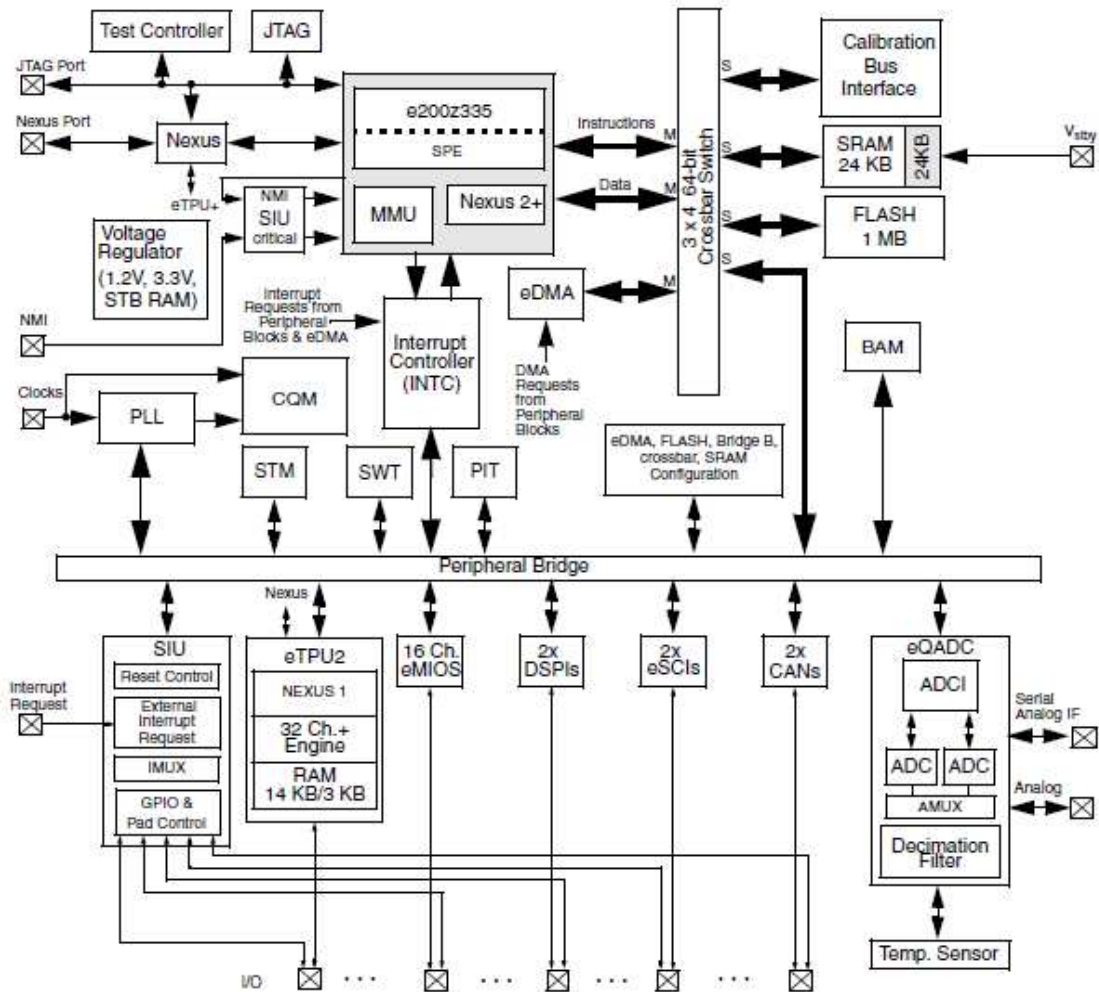


Figure 4-3: MPC5632M block diagram [6]

4.2.1 1.2 V Power Supply for the Microcontroller

The microcontroller has a 5 V single power supply. Internal regulators provide 3.3 V for the core and 1.2 V is provided to the core using an external transistor. Figure 4-4 shows the schematic of the internal regulator that provides 1.2 V (VDD) for the core.

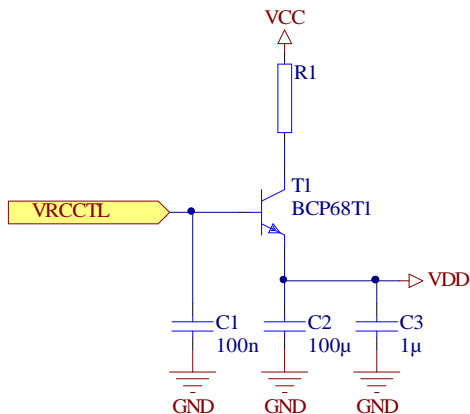


Figure 4-4: Schematic with internal regulator to provide 1.2 V (VDD) for the core

An internal regulator, V_{RCCLT} , and an external bypass transistor are used to provide 1.2 V to the core. The bypass transistor must be operated outside of the saturation region. For maximum transient performance [6], the recommended bypass capacitor for each pin that supplies the digital core is 20uF - 100uF with very low ESR (max 10 m Ω). A ceramic capacitor is also desirable, with 200 nF to 1uF capacitance, see Figure 4-4. Current which can be sourced by V_{RCCTL} is 7.5 mA at 150°C and 11 mA at -40°C; the maximum operating current for the VDD is 250 mA.

The transistor BCP68T1 [9] has a minimum DC current gain, $h_{FE} = 50$, maximum power dissipation $P_D = 0.78$ W at +85°C ambient temperature and a thermal resistance $R_{\theta JA} = 83.3^\circ\text{C/W}$, a maximum operating junction temperature $T_j = 150^\circ\text{C}$ and a maximum collector-emitter saturation voltage $V_{CE} = 0.5$ V, see Table 4.1.

Table 4.1: Specification for the transistor BCP68T1

h_{FEmin}	P_D [W]	$R_{\theta JA}$ [$^\circ\text{C/W}$]	T_j [$^\circ\text{C}$]	$V_{CESATmax}$ [V]
50	0.78	83.3	150	0.5

The power dissipation in the transistor without a collector resistor is

$$P = V_{CE} \cdot I_C = (V_{CC} - V_{DD}) \cdot I_C = (5 - 1.2) \cdot 0.25 = 0.95 \text{ W} \quad (1)$$

which is above the maximum power dissipation for BCP68T1 at +85°C and yields a junction temperature of

$$T_j = P \cdot R_{\theta JA} + T_A = 0.95 \cdot 83.3 + 85 = 164^\circ\text{C} \quad (2)$$

which also is too high. Therefore a collector resistance is needed, see Figure 4-4.

The transistor must not be saturated and therefore the maximum resistor is

$$R_{max} = \frac{V_R}{I_{Cmax}} = \frac{V_{CC} - V_{CEsat} - V_{DD}}{I_{Cmax}} = \frac{5 - 0.5 - 1.2}{0.25} = 13.2 \Omega \quad (3)$$

The maximum power dissipation in a 13.2 Ω resistor is 0.825 W, see Figure 4-4, and the power dissipation in the transistor is reduced to a minimum when a maximum value of the resistor is used. The power dissipation is divided equally between the resistor and transistor at maximum current when the resistance is

$$R = \frac{V_R}{I_{Cmax}} = \frac{V_{CC} - V_{DD}}{2 I_{Cmax}} = \frac{5 - 1.2}{2 \cdot 0.25} = 7.6 \Omega \quad (4)$$

The chosen collector resistance is therefore 7.5 Ω which is the closest value in the E24 series. The maximum power dissipation in the 7.5 Ω resistor is 0.47 W and the maximum power dissipation in the transistor is 0.48 W which yields an acceptable maximum junction temperature of 125°C.

4.2.2 Crystal Oscillator

The Frequency-Modulated Phase Locked Loop (FMPLL), see Figure 4-3, allows the user to generate high speed system clocks from any 4 MHz to 20 MHz crystal. An 8 MHz quartz crystal was chosen of type 92M080-16(D) [10] manufactured by SMI.

4.2.3 Programming the Microcontroller

MPC5632M has a Boot Assist Module (BAM) which is a block of read-only memory that is programmed once by Freescale. The BAM program is executed every time the microcontroller unit is powered-on or reset in normal mode and can be used to program the microcontroller.

Another way, which is used in this design, of programming the microcontroller is with a boot code. The boot code is written to the boot sector in the flash by using the JTAG interface. Self-programming or in-system programming capability is achieved by utilizing a boot sector in the flash memory. When executing the boot code the microcontroller can receive new code via a serial communication channel, for instance CAN, and can program that code into its own flash program memory.

4.2.4 Input and Output Signals

Not all the different blocks in the microcontroller are used. The main blocks used are the ADC, eTPU2, GPIO and CAN, see Figure 4-3.

- The AD converter in the microcontroller is used for measuring the injector current in the CM and the signals from the piezoelectric vibration sensors in the KM.
- The eTPU2 is used for the engine position signals in both CM and KM. It is also used in the CM for controlling the injector drivers and the ignition units.
- Four rotary switches [11] are connected to the GPIO of the microcontroller, see Figure 4-5. Two switches indicate the number of cylinders in the engine, one switch indicates the unit digit and one the decade digit. The other two switches indicate the engine type and the CM position on the engine.

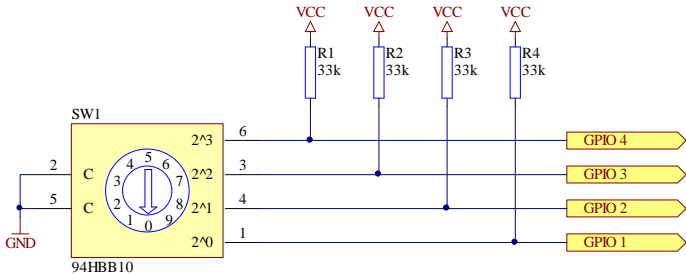


Figure 4-5: Rotary switch used to identify the CM

4.3 Main CC and PCC Injectors - CM

The MC supplies fueling data to the CM via the CAN bus. The CM receives amplified crank and cam signals from the KM and activates the fuel injection relative to the cylinder top dead center (TDC) according to information from the MC. Each cylinder has a main and a PCC injector. Different engine types have different injectors, see Table 4.2, so the pull-in time, pull-in current, hold time and hold current, see Figure 4-6, differs from type to type. The ambient temperature is maximum +85°C and a fuel injector driver must be chosen so that the power loss will be small and the junction temperature is kept below the specified limit. The maximum engine speed is 1800 rpm.

When designing an injector driver it is important to calculate the power dissipation in the components and the signal delay they introduce. Figure 4-6 shows the current and time definitions for the injectors. The temporary current increase in the slope just after the pull-in phase occurs when the plunge stops at the end of its movement.

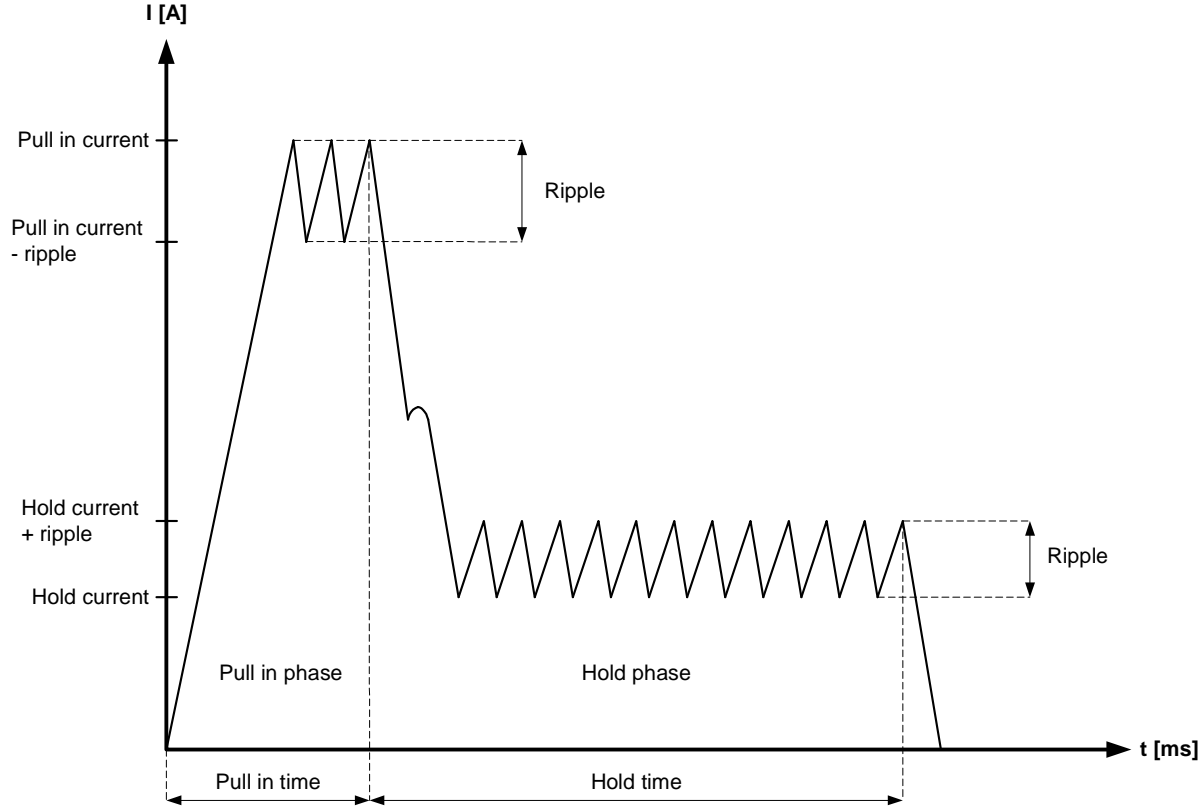


Figure 4-6: Injector current and time definitions

The inductance and resistance values in Table 4.2 are measured with an ISO-Tech LCR819 LCR meter and an HP 34401A multimeter. SOGAV 105 and SOGAV 43 [12] are the main injectors and SOGAV 2.2 [13] and Servo Jet SP 021 are the PCC injectors.

Table 4.2: Measured inductance and resistance for the injector valves

Injector	L [mH]				R [Ω]
	f = 100 Hz	f = 1 kHz	f = 10 kHz	f = 100 kHz	
SOGAV 105	5.7284	3.6426	2.256	1.5795	1.0
SOGAV 43	9.1258	6.6641	4.1812	2.8886	1.9
SOGAV 2.2	7.8985	3.0002	1.2702	0.6979	2.7
SERVO JET SP 021	9.5114	4.5252	1.5607	0.65198	1.6

4.3.1 Freewheeling and Clamping

Figure 4-7 shows the two main methods, clamping and freewheeling, used when switching an inductive load. The freewheeling method is the slower of the two but it also causes less power dissipation in the transistor. The higher power dissipation in the transistor when the clamping method is used is due to the high drain-source voltage when the transistor is turned off. The load on the transistor is therefore much higher when the clamping method is used. When the transistor is turned off, the inductor voltage increases and therefore also the drain-source voltage. When it exceeds the value of the zener diode connected between the drain and gate, see Figure 4-7, the transistor is turned on again. This happens almost instantaneously and the inductor current is therefore never turned off, see Figure 4-10. The inductor current decreases through the transistor until it reaches zero and then the gate voltage decreases which causes the transistor to turn off. The drain-source voltage is high while the inductor current decreases.

The clamping method turns off the injector faster because the inductor voltage is higher compared to when a freewheeling diode is used, see Figure 4-12 and Figure 4-14. The power peak in the transistor is high during turn off, see Figure 4-14. The time depends on the inductance of the injector and the injector voltage. The maximum allowed injector voltage is limited by the drain-source breakdown voltage of the transistor.

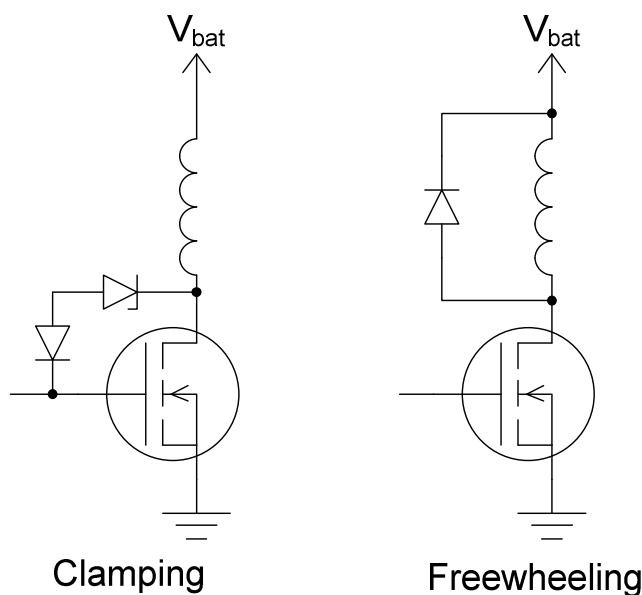


Figure 4-7: Simplified schematic of freewheeling and clamping methods

Figure 4-8 shows the current through the transistor when a freewheeling diode is used. The current goes through the freewheeling diode when the transistor is turned off. Figure 4-9 shows the current through the freewheeling diode.

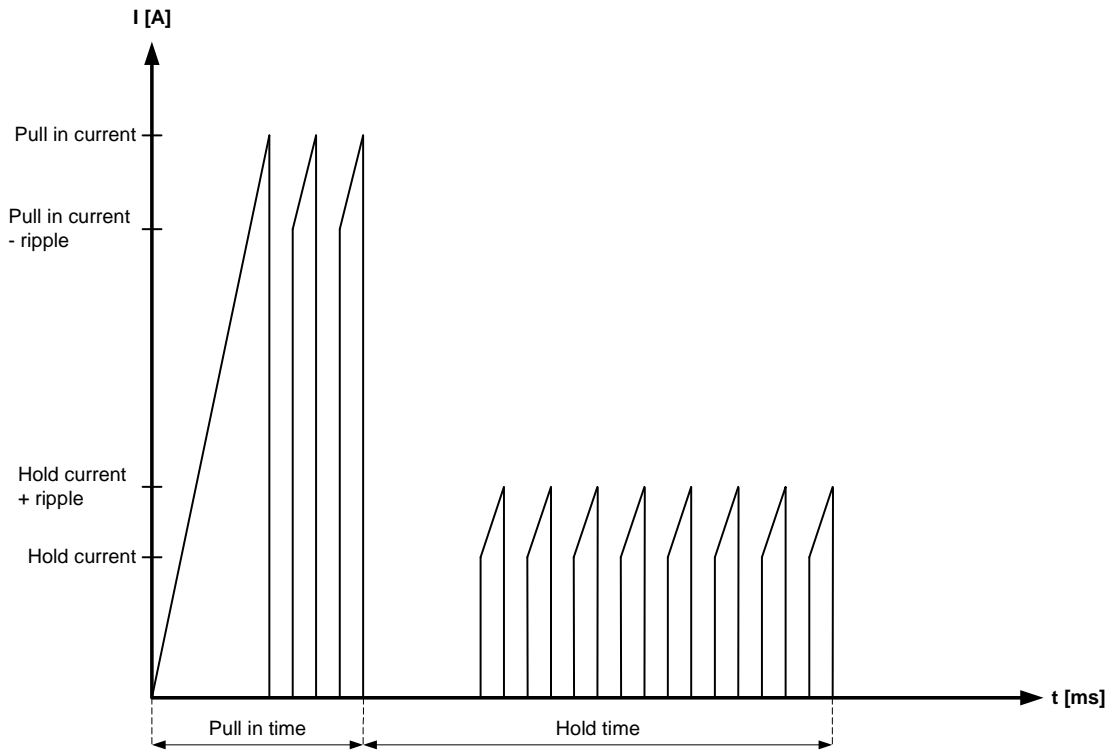


Figure 4-8: Current through the transistor when a freewheeling diode is used

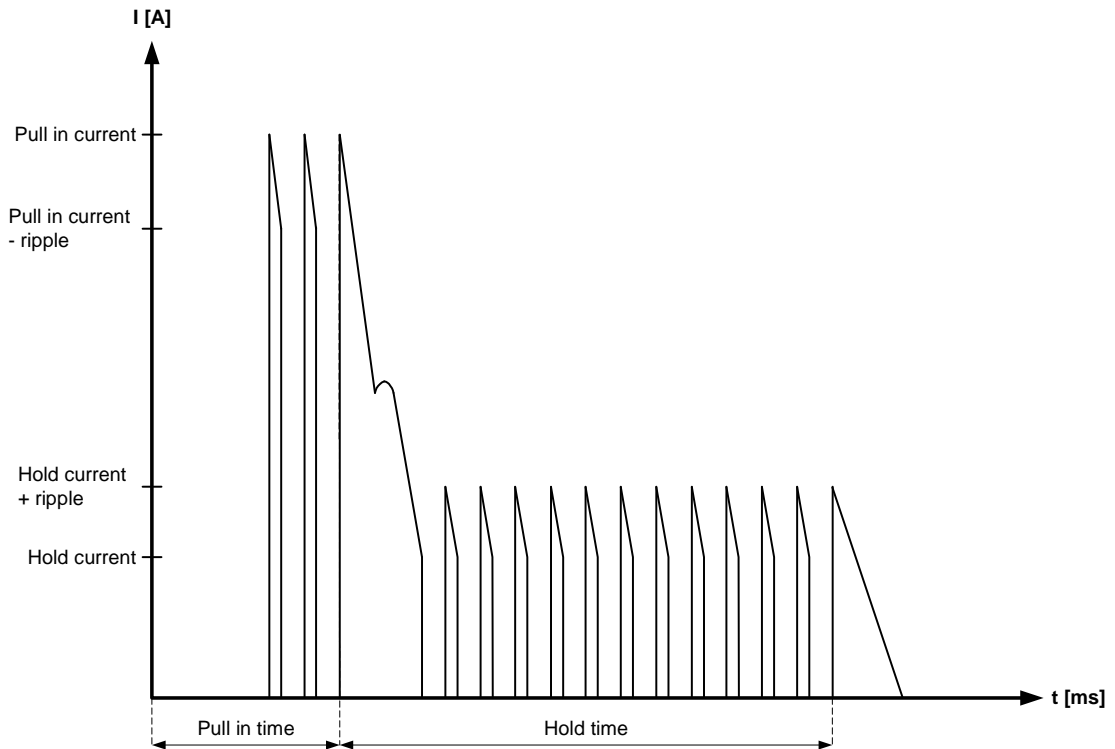


Figure 4-9: Current through the freewheeling diode

Figure 4-10 shows a simulation of a clamping circuit. The blue line is the inductor current, the green is the gate voltage and the pink is the drain-source voltage.

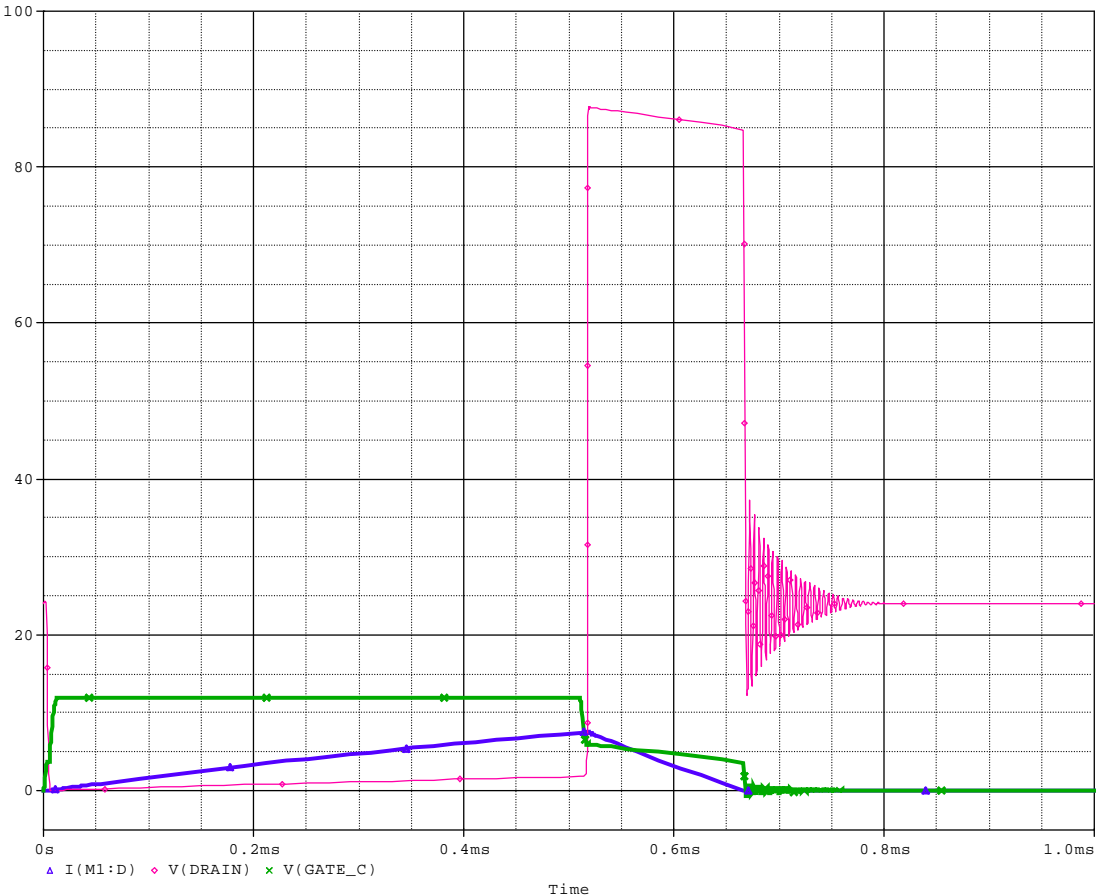


Figure 4-10: Simulation in OrCAD of a clamping circuit. Inductor current - blue, gate voltage - green, drain-source voltage - pink

Figure 4-11 shows a simulation of a circuit with a freewheeling diode. The blue line is the inductor current, the orange is the current through the freewheeling diode, the green is the gate voltage and the pink is the drain-source voltage.

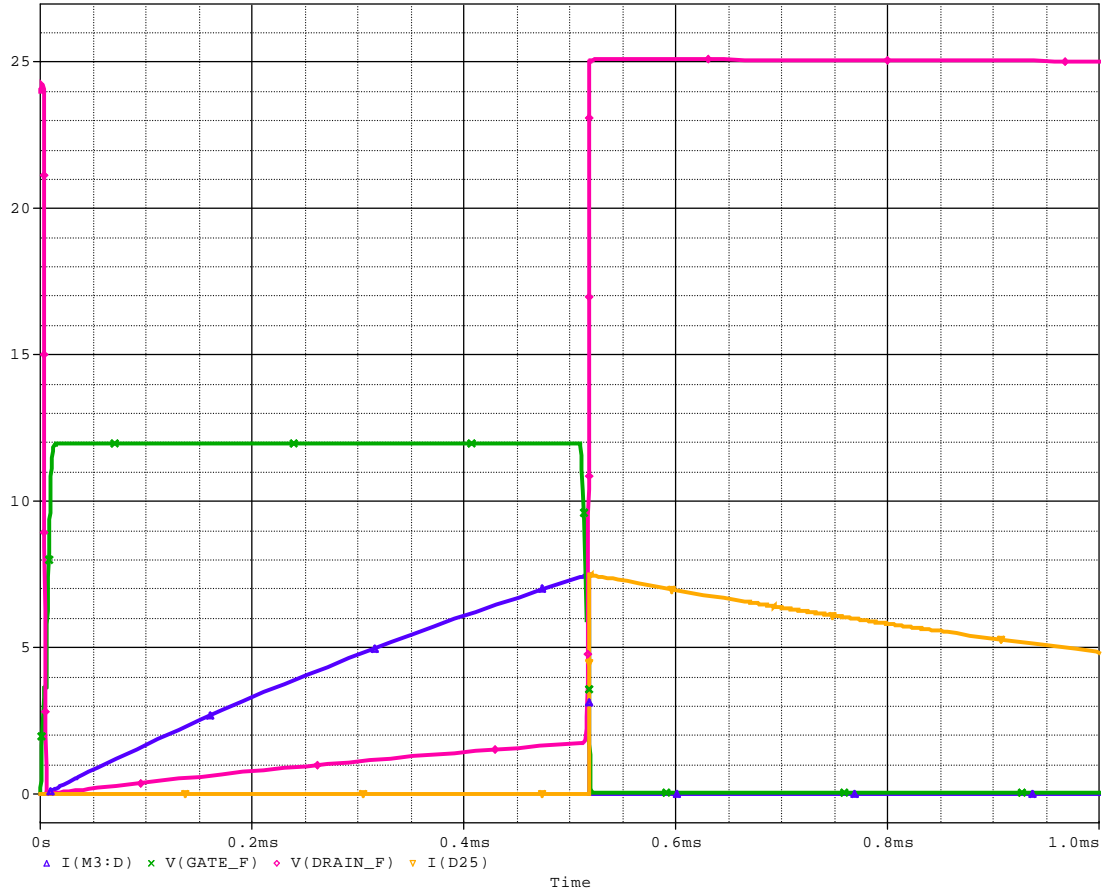


Figure 4-11: Simulation in OrCAD with a freewheeling circuit. Inductor current - blue, freewheeling diode current – orange, gate voltage - green, drain-source voltage - red

The difference in turn-off time and drain-source voltage between the clamping method and freewheeling can be seen in Figure 4-10, Figure 4-11 and Figure 4-12.

Figure 4-12 shows a simulation of the inductor current with a freewheeling diode in red and with the clamping method in blue.

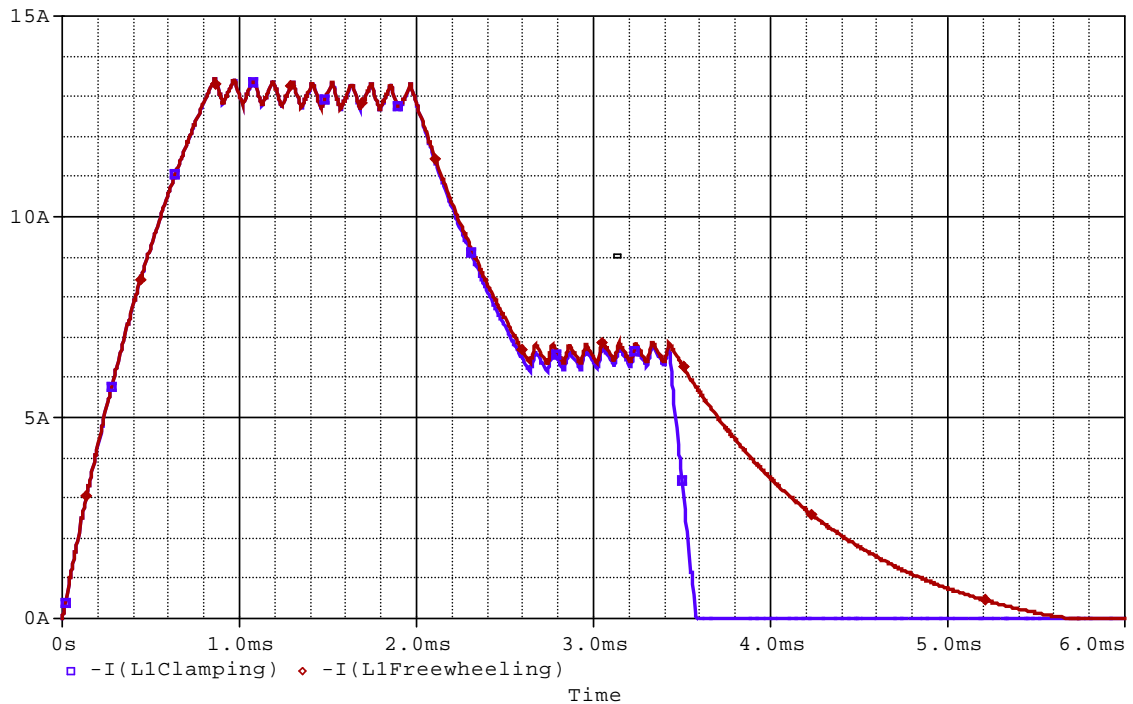


Figure 4-12: Inductor current simulation in OrCAD. Freewheeling diode - red, clamping - blue

When the clamping method is used the current is controlled by the high side drive (HSD) transistor and the low side drive (LSD) transistor is turned on constantly until the injector is turned off, see Figure 4-13. The injector is turned off after approximately 3.4 ms in Figure 4-14 and the simulation shows that the turn off time is much shorter for the clamping method compared to the freewheeling method. The high inductor voltage causes the shorter turn off time. A high inductor voltage leads to a high drain-source voltage and therefore the power dissipation is very high at turn off. This can be seen in Figure 4-14.

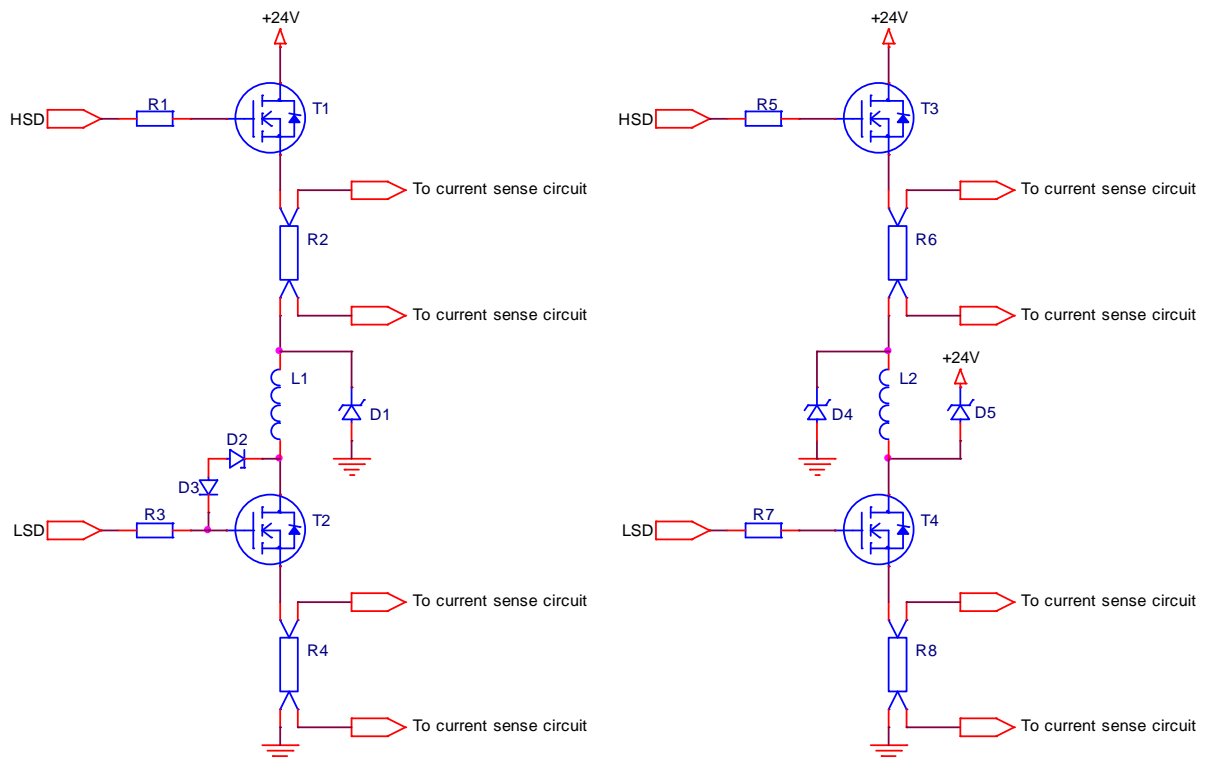


Figure 4-13: Simplified schematic of HSD and LSD with the clamping method to the left and the freewheeling method to the right.

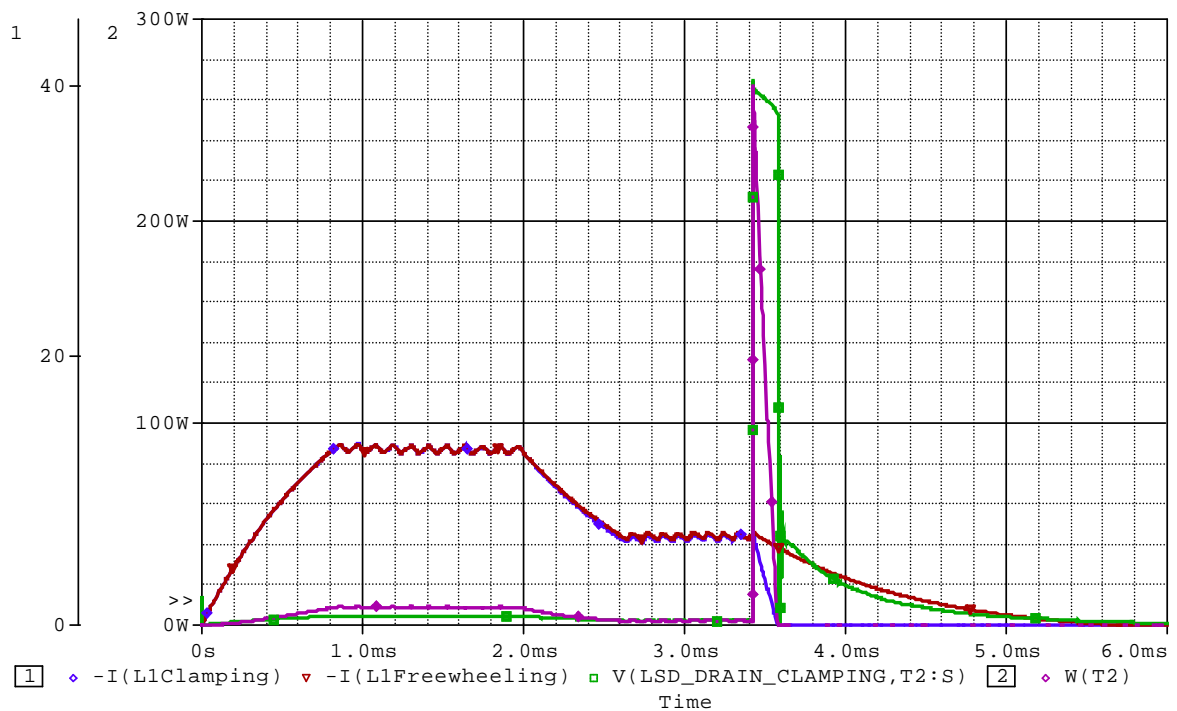


Figure 4-14: Injector current control with the clamping and freewheeling methods. Injector current clamping – blue, injector current freewheeling – red, drain-source voltage over the clamping transistor – green and power dissipation in the clamping transistor – purple.

4.3.2 Power Loss in the Injector Drive Transistor

As stated earlier, it is important to calculate the power dissipation in all power components so that the junction temperature does not exceed the specified limit. The total power loss in the injector drive transistor is

$$P_{tot} = P_c + P_{sw} \quad (5)$$

where P_c is the conduction loss and P_{sw} is the switch loss.

The switch loss, P_{sw} is approximately

$$P_{sw} = \left(\frac{V \cdot I_{pull} \cdot t_r}{2} + \frac{V \cdot I_{pull} \cdot t_f}{2} + \frac{V \cdot I_{hold} \cdot t_r}{2} + \frac{V \cdot I_{hold} \cdot t_f}{2} \right) \cdot f \cdot \frac{t_{on}}{T} \quad (6)$$

where V is the drain-source voltage, I_{pull} and I_{hold} are the currents through the transistor during the pull and hold phases, f is the switching frequency, t_{on} is the maximum time the injector is activated, T is the period and t_r is the rise time and t_f is the fall time of the transistor gate voltage.

The conduction loss, P_c is

$$P_c = R_{DSon} \cdot I_{RMS}^2 \quad (7)$$

where R_{DSon} is the on-resistance and I_{RMS} is the RMS current of the transistor.

The combustion frequency, f_c per cylinder for a four stroke engine is

$$f_c = \frac{\text{engine speed in rpm}}{2 \cdot 60} \quad \Rightarrow \quad T = \frac{2 \cdot 60}{\text{engine speed in rpm}} \quad (8)$$

and the definition of the RMS current, I_{RMS} in a fuel injector driver is

$$I_{RMS} = \sqrt{\frac{1}{T} \cdot \int_0^T i^2 dt} \quad \text{which yields} \quad (9)$$

$$I_{RMS} = \sqrt{\frac{1}{T} \cdot (I_{pull}^2 \cdot t_{pull} \cdot D_{psw} + I_{hold}^2 \cdot t_{hold} \cdot D_{hsw})} \quad (10)$$

where I_{pull} is the pull-in current, t_{pull} is the pull-in time, D_{psw} is the switching duty cycle during pull-in phase, I_{hold} is the hold current, t_{hold} is the hold time and D_{hsw} is the switching duty cycle during hold phase.

According to the specification the maximum time that the injector can be activated is 65 ms. The time for the hold current is calculated as the maximum activated time minus the pull-in time. The switch duty cycle depends on the inductance in the injector, voltage across the injector and losses in the circuit. Worst case conditions are always used.

Calculating the exact junction temperature for a component is impossible. Instead approximations are used. The average junction temperature, T_j can be approximated [16] by the equation

$$T_j = R_{thJA} \cdot P_{tot} + T_a \quad (11)$$

where the R_{thJA} is the junction-ambient thermal resistance, P_{tot} is the total power and T_a is the ambient temperature.

This calculation is a good approximation of the average junction temperature when a freewheeling diode, see Figure 4-7, is used to prevent the voltage over the transistor from increasing above the supply voltage. The inductor current flows through the freewheeling diode when the gate voltage is set low to turn the transistor off.

A transistor drain-source voltage of 90 V and an injector current of 7 A creates a 630 W power peak in the transistor. The power peak temporarily increases the junction temperature [16] above the average junction temperature. All semiconductors have a pulse power limit that must be taken into account especially when using the clamping method. For this reason a freewheeling diode was used in this design. The turn off time is not critical in this design.

Table 4.3 shows the power and temperature calculations for the freewheeling method with the OptiMOS 2 power-transistor IPB05CN10N G [14] as a fuel injector driver according to equations (5) – (11). The maximum time for the injector to be activated is 65 ms, which is the sum of the pull-in time and the hold time.

Table 4.3: Power and temperature calculations for the injector driver using freewheeling diode for different engines

Main/PCC	Pull-in time [ms]	Pull-in current [A]	Hold current [A]	I_{rms} [A]	P_C [W]	P_{sw} [W]	P_{tot} [W]	T_j [°C]
Main	6.3	7.8	2.9	1.91	0.019	0.019	0.038	87.3
PCC	3.2	4.7	1.6	0.98	0.005	0.011	0.016	86.0
Main	6.3	7.8	2.9	2.56	0.033	0.034	0.067	89.2
PCC	3.2	4.7	1.6	1.31	0.009	0.020	0.029	86.8
Main	7.0	12.6	5.9	3.61	0.066	0.032	0.098	91.1
PCC	2.0	13.7	6.7	3.65	0.068	0.035	0.103	91.4
Main	7.0	12.6	5.9	3.61	0.066	0.032	0.098	91.1
PCC	3.2	4.7	1.6	0.98	0.005	0.011	0.016	86.0

According to the datasheet [14], the maximum rise time, t_r and fall time, t_f of the transistor gate voltage are $t_r = 63$ ns and $t_f = 31$ ns. But those values are measured with $R_g = 1.6$ Ω , $V_{DD} = 50$ V, $V_{GS} = 10$ V and $I_D = 50$ A. The datasheet does not specify how these times vary as a function of the gate resistor value. The rise and fall times will increase when a higher gate resistor is used which means that the switching losses are too low in Table 4.3. With rise and fall times as high as 1 μ s, see Table 4.7, the maximum junction temperature will be 130°C instead of 91°C. However, as the absolute maximum operating temperature of the IPB05CN10N G transistor is 175°C it can be used in this injector driver circuit.

Table 4.4: Power and temperature calculations for the injector driver using the clamping method for different engines

Main/PCC	Pull-in time [ms]	Pull-in current [A]	Hold current [A]	P_C [W]	P_{sw} [W]	P_{tot} [W]	T_j [°C]
Main	6.3	7.8	2.9	0.23	0.00	0.23	99.3
PCC	3.2	4.7	1.6	0.12	0.00	0.12	92.2
Main	6.3	7.8	2.9	0.42	0.00	0.42	110.7
PCC	3.2	4.7	1.6	0.21	0.00	0.21	98.0
Main	7.0	12.6	5.9	0.53	0.00	0.53	117.6
PCC	2.0	13.7	6.7	0.58	0.00	0.58	121.1
Main	7.0	12.6	5.9	0.53	0.00	0.53	117.6
PCC	3.2	4.7	1.6	0.12	0.00	0.12	92.2

The power dissipation in the transistor is higher when the clamping method is used than when a freewheeling diode is used, see Table 4.3 and Table 4.4.

4.3.3 Power Loss in the Freewheeling Diode

The power loss in the freewheeling diode is

$$P = V_F \cdot I_{FAVG} \quad (12)$$

where V_F is the forward voltage drop and I_{FAVG} is the average forward current through the diode. The average forward current is defined as

$$I_{AVG} = \frac{1}{T} \cdot \int_0^T i(t) dt \quad (13)$$

where T is the time for one complete period and $i(t)$ is the injector current. Using the approximation that the current is a square wave, compare Figure 4-9, the average current through the freewheeling diode is

$$I_{AVG} = D \cdot \frac{1}{T} \cdot (I_{Pull} \cdot t_{pull} + I_{Hold} \cdot t_{Hold}) \quad (14)$$

where D is the duty cycle, T is the time period, I_{pull} is the pull-in current, t_{pull} is the pull-in time, I_{hold} is the hold current and t_{hold} is the hold time.

Table 4.5 shows the power and temperature calculations with the diode 12CWQ10FNPbF [15] as a freewheeling diode and when a duty cycle of 50% is used. Equations (11) and (14) are used in the calculations.

Table 4.5: Power and temperature calculations for the freewheeling diode for different engines

Main/PCC	Pull-in time [ms]	Pull-in current [A]	Hold current [A]	I_{AVG} [A]	P [W]	T_j [°C]
Main	6.3	7.8	2.9	0.91	0.59	86.1
PCC	3.2	4.7	1.6	0.47	0.31	85.6
Main	6.3	7.8	2.9	1.65	1.07	86.9
PCC	3.2	4.7	1.6	0.85	0.56	86.0
Main	7.0	12.6	5.9	1.79	1.17	87.1
PCC	2.0	13.7	6.7	1.87	1.22	87.2
Main	7.0	12.6	5.9	1.79	1.17	87.1
PCC	3.2	4.7	1.6	0.47	0.31	85.6

4.3.4 Current Sensing

The current through the injector is measured with a current sensing resistor, see Figure 4-15. Some current sense resistors have 4 terminals to increase the accuracy of the measurement. CSM3637 [17] from Vishay is one of those resistors.

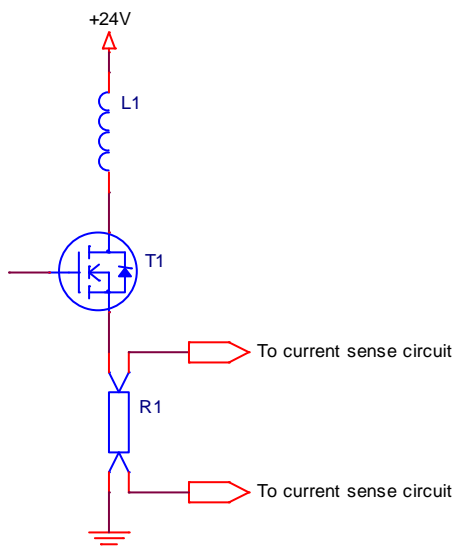


Figure 4-15: Current sensing

The minimum injector hold current is 1.6 A and the maximum injector pull-in current is 13.7 A, see Table 4.3. The injector current can for instance be measured with a differential amplifier or with a high voltage current shunt monitor circuit like AD8210 [18] which is used in this design. It has a gain of 20 times, a maximum output voltage of 4.9 V and the maximum input voltage is therefore 250 mV. The maximum resistance of the current sensing resistor is

$$R = \frac{U}{I} = \frac{0.25}{13.7} = 18 \text{ m}\Omega \quad (15)$$

The current sensing resistor is chosen to 15 mΩ which yields a maximum current of 16.7 A. The maximum RMS current is 3.65 A according to Table 4.3 which yields a power loss of only 0.2 W in a 15 mΩ resistor. When the input voltage is equal to or higher than 250 mV the output voltage from the AD8210 circuit is 4.9 V. With a 12 bit AD converter and a 15 mΩ current resistor the current quantization steps are only $\frac{16.7}{2^{12}} = 4.1 \text{ mA}$. The injector current ripple, see Figure 4-6, is about 0.5 A and it is therefore possible to use the same current resistor for all the different injector types that are used.

4.3.5 Protection from Short Circuit Connection

The injector driver must be protected from short circuit connection. A short circuit occurs when the outputs by accident become connected to the supply voltage or ground instead of to the injector. With the MOSFET IPB05CN10N G [14] this means that a 50 A current can go through the transistor for 1 ms, almost 200 A for 100 μs or 400 A for 10 μs before the current is turned off by the transistor. A thyristor has a turn on time of roughly a few microseconds so a thyristor is used to turn off the transistor if the current is too high, see Table 4.7. A thyristor has a large spread on the gate trigger voltage (V_{gt}) and normally it is only the maximum V_{gt} which is specified in the datasheets. But due to physical laws, among others the band gap for semiconductors, the minimum V_{gt} is about 0.3 V. The maximum V_{gt} for the thyristor NYC0102BLT1G [19] is 1 V at -40°C, the gate trigger current is 200 μA and the maximum hold current is 6 mA. The value of the gate resistor of the transistor, R1 in Figure 4-16, sets the hold current to the thyristor and the maximum current allowed through the transistor can be adjusted with the thyristor gate resistors, R2 and R3 in Figure 4-16. Without a gate cathode resistor, R2 in Figure 4-16, the spread of the maximum allowed injector current is

$$I = \frac{V_{gt}}{R_4} \quad (16)$$

which yields 20 A for a V_{gt} of 0.3 V and 67 A for a V_{gt} of 1 V.

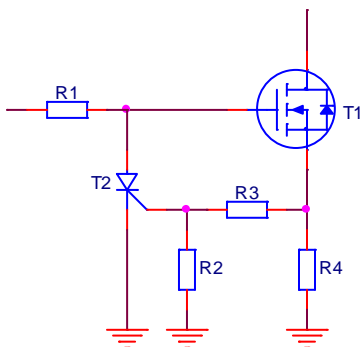


Figure 4-16: Protection from short circuit connection using a thyristor

With a voltage divider as in Figure 4-16 the turn off current is

$$I = \frac{(R_2 + R_3)}{R_2 \cdot R_4} \cdot V_{gt} \quad (17)$$

The turn on and turn off delay of the transistor is calculated from

$$V_C(t) = V \cdot \left(1 - e^{-\frac{t}{R_g \cdot C_p}} \right) \quad (18)$$

where V is the maximum gate voltage, R_g is the gate resistor and C_p is the parasitic input capacitance in the transistor.

Table 4.7 shows the maximum and minimum turn off currents with different voltage divider resistors, R_2 and R_3 . It also shows the power in the gate resistor, R_1 and the turn on and off time of the MOSFET due to the parasitic input capacitance, C_p . A current sense resistor of 15 m Ω is used in the calculations. The values in Table 4.7 have been calculated using the values in Table 4.6 which have been taken from the datasheets for the components.

Table 4.6: Maximum and minimum component values from datasheets

NYC0102BLT1G [19]		IPB05CN10N G [14]		MC7812B [41]	
V_{gtmin} [V]	V_{gtmax} [V]	$V_{GS(th)max}$ [V]	C_{pmax} [nF]	V_{omin} [V]	V_{omax} [V]
0.3	1	4	12	11.5	12.5

Table 4.7: Protection from short circuit connection using a thyristor

R_1 [k Ω]	R_2 [k Ω]	R_3 [k Ω]	P_{R1} [W]	I_{T2} [mA]	t_{onT1} [μ s]	I_{min} [A]	I_{max} [A]
0.18	100	1	0.87	69	0.9	20	54
0.22	47	1	0.71	57	1.1	20	68
0.51	10	1	0.31	25	2.6	22	73
0.68	5.1	1	0.23	18	3.5	24	80
1	2.7	1	0.16	13	5.1	27	91

Table 4.7 shows the worst case values. The power in the gate resistor, R_1 increases linearly and the turn on and turn off times decrease almost linearly with the decrease of the resistor value. Therefore a trade off between delay and power dissipation in the transistor must be done. The current ripple in the injectors can be between 0.5 – 1 A depending on the injector type. The switching time is approximately 50 μ s and a 1 μ s delay is well within limits. An optional transistor with less than half the input capacitance and lower gate threshold voltage is IPB081N06L3 G [20]. IPB081N06L3 G has a slightly higher R_{DSon} and the rise and fall times are shorter. The total power loss and junction temperature is therefore almost the same.

A high side and a low side driver are used to protect the injector driver in case of a short circuit connection, see Figure 4-18. IR2181 [21] is a high voltage, high speed power MOSFET driver with independent high and low side referenced output channels.

IR2181 is therefore used to drive both the high-side and the low-side MOSFET components. IR2181 has typically a 40 ns turn on time, typically a 20 ns turn off time and a typical output source and sink current capability of 1.4A and 1.8A respectively. The power supply is 12 V and the supply current is

$$I = C_p \cdot \frac{dV}{dt} \quad (19)$$

where C_p is the input capacitance for the MOSFET and $\frac{dV}{dt}$ is the slew rate for IR2181.

A capacitance of 12 nF and a turn on slew rate of 300 V/ μ s yield a source current of 3.6 A which is more than what IR2181 can supply. This means that the turn on time will be limited by the maximum output source current for the IR2128 and not by the transistor. The maximum sink current is with the same reasoning as for the source current 7.2 A which also is more than what the IR2181 can sink and the turn off slew rate is also limited by the maximum output sink current for the IR2128. But the current is also limited by the series gate resistance and the maximum gate current due to the series resistance is

$$I_{max} = \frac{V}{R_g} \quad (20)$$

where R_g is the gate resistance and V is the voltage from the MOSFET driver. The gate current decreases exponentially according to

$$I_g(t) = \frac{V \cdot e^{-\frac{t}{R_g \cdot C_p}}}{R_g} \quad (21)$$

where V is the voltage from the MOSFET driver, R_g is the gate resistance and C_p is the input capacitance for the MOSFET.

The maximum gate current is limited by the 180 Ω gate resistance to 67 mA according to equation (20).

Figure 4-17 and Figure 4-18 show the schematic of the injector driver using freewheeling diodes and the clamping method respectively. Both circuits are protected from short circuit connection by a thyristor.

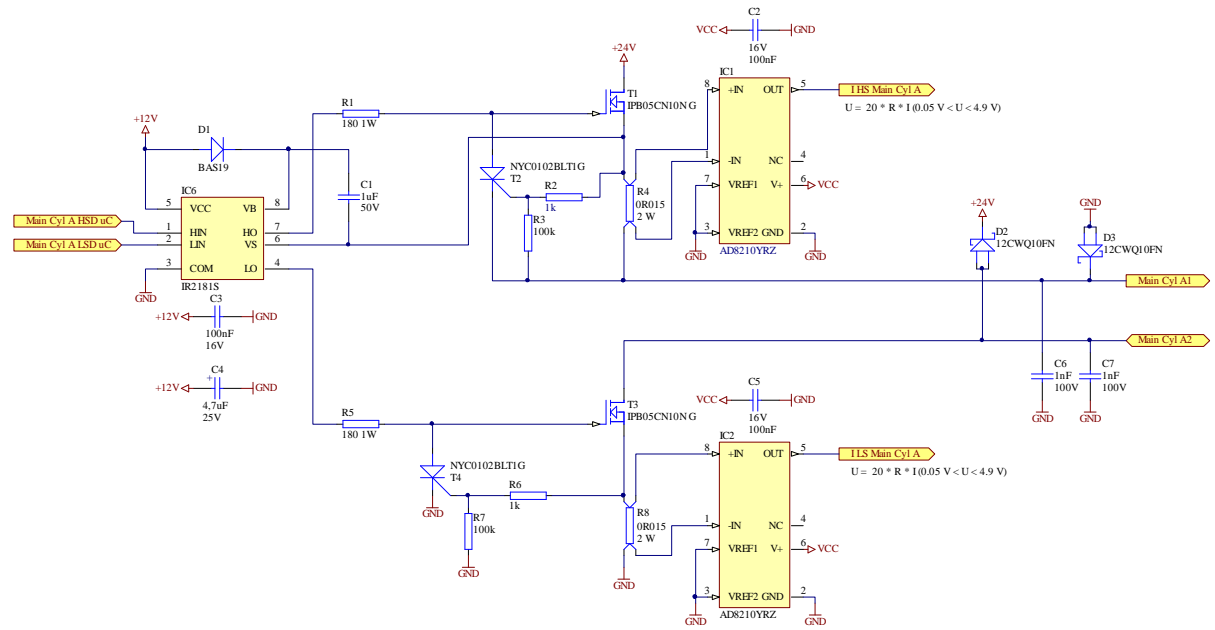


Figure 4-17: Injector driver using freewheeling diodes protected from short circuit connection

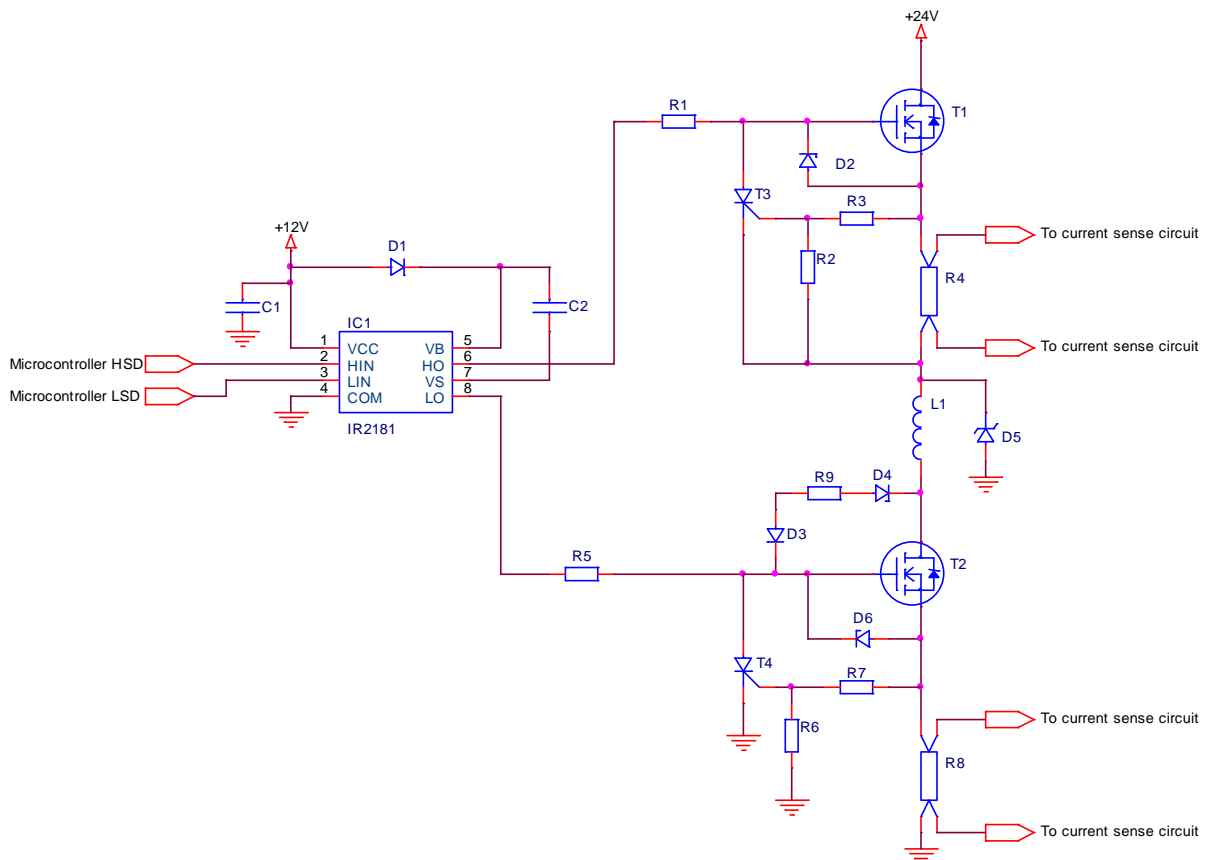


Figure 4-18: Injector driver using the clamping method protected from short circuit connection

4.4 Ignition Timing - CM

The MC determines the ignition timing from the data it receives from different engine units. The MC supplies ignition timing data to the CM via the CAN bus. The CM receives crank and cam signals and activates the spark delivery at the engine position determined by the MC. This is done by pulling a signal to the ignition unit low, see Figure 4-19.

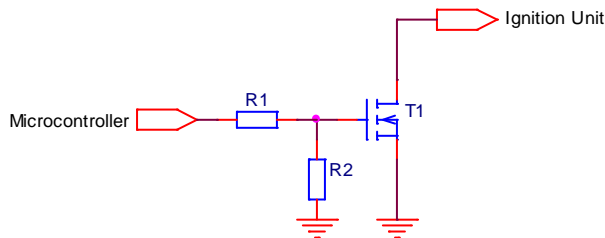


Figure 4-19: Schematic of the spark delivery activation

4.5 CAN - CM and KM

All communication between the different units controlling the engine is done over a CAN bus. The KM sends knock information to the MC. The MC transmits commands with requested ignition timing, ignition voltage, fuel timing and fuel amount to all CM units.

There are many different CAN transceiver integrated circuits that can be used for CAN communication, TLE6250 [22] and TJA1040 [23] are two of them. TJA1040 is used in this design. The CAN unit in the microcontroller is connected to a CAN transceiver with appropriate external components [24], see Figure 4-20. The filtered output signals from the CAN transceiver are connected to the CAN bus. A yellow LED controlled by the microcontroller indicates if the CAN communication is working correctly, see Figure 4-21.

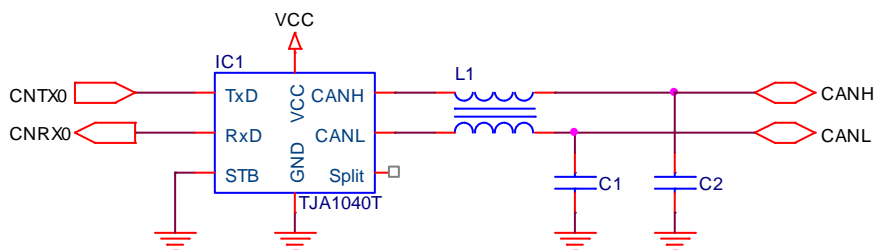


Figure 4-20: Schematic of the CAN interface

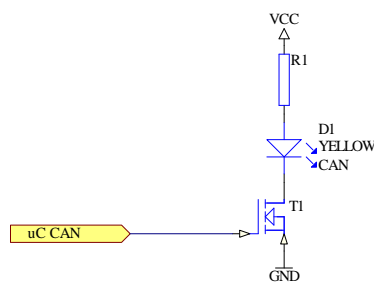


Figure 4-21: Schematic of the indication with a LED of correct operation of the CAN communication

4.6 Thermocouples - CM

The CM has two K-type temperature sensors for each cylinder. They measure the exhaust gas temperature with a range from 0° to 1000°C. The thermocouple inputs of K-type (chromel - alumel) have a sensitivity of only approximately 41 $\mu\text{V}/^\circ\text{C}$ so the signal must be amplified. The temperature is continuously monitored and the result is transferred by the microcontroller over the CAN bus to the MC.

Maxim has an integrated circuit called MAX6675 [25] which is a cold-junction-compensated K-thermocouple-to-digital converter. It is very easy to use and it measures temperatures from 0°C to 1024°C. The temperature is transferred digitally to the microcontroller on a SPI interface. But the operational temperature range for MAX6675 is only -20°C to +85°C so it can only be used after agreement with the customer.

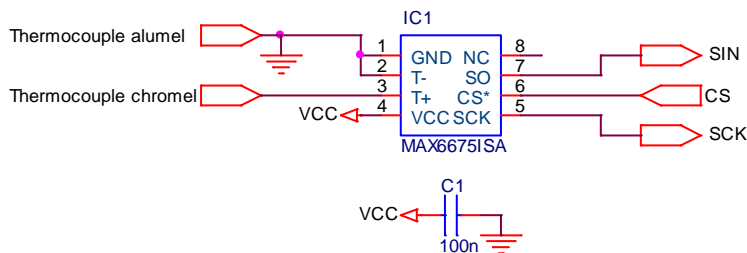


Figure 4-22: Schematic of thermocouple inputs using MAX6675ISA

Analog Device has an integrated circuit called AD595 [26] which is a monolithic thermocouple amplifier with cold junction compensation. The operational temperature range is -55°C to +125° and it can measure temperatures from -200°C to +1250°C, the range depends on the supply voltage. When a single supply of +10 V is used the measuring range is from 0° to almost 1000°C.

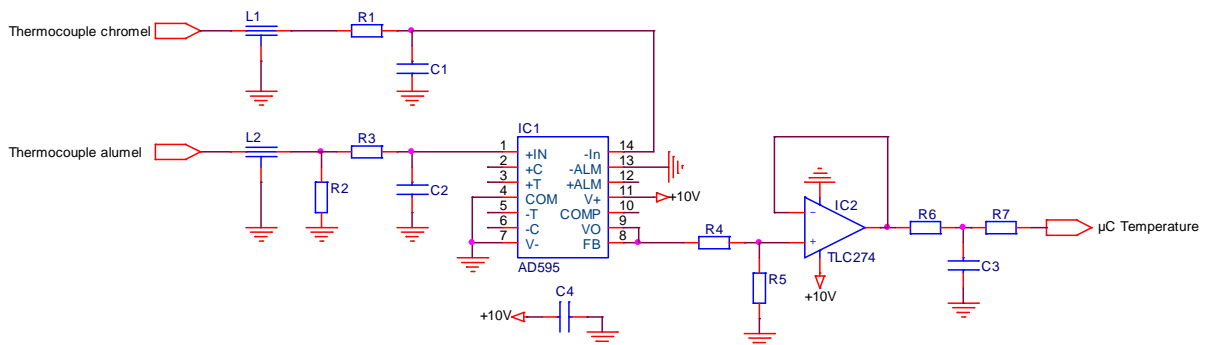


Figure 4-23: Schematic of thermocouple inputs using AD595

The output voltage from the AD595 is an analog signal and the maximum voltage is the same as the supply voltage, +10 V in this design. The signal is therefore reduced to maximum 5 V with R4 and R5 and connected to a voltage follower, see Figure 4-23. The output signal from the voltage follower is filtered and connected to the AD converter in the microcontroller. TLC274 [27] is a precision unity stable operational amplifier which is used as a voltage follower.

4.7 Engine Position Signals - CM and KM

The crankshaft, sometimes abbreviated as the crank, is the part of an engine which translates reciprocating linear piston motion into rotation. The crank sensor monitors the position of the crankshaft. The crank sensor is used in combination with the similar camshaft position sensor to monitor the relationship between the pistons and valves in the engine. The engine position is consequently detected by the crank and cam signals and that information is used by the engine to control ignition system timing and other engine parameters.

In the EMS engines the crank position pulse train consists of 900 pulses per two engine revolutions and the cam shaft position indicator is one pulse per engine cycle which is two revolutions in a four stroke engine. Figure 4-24 shows a Wärtsilä 34SG engine, the large flywheel at the front of the picture resists changes in the rotational speed and therefore stabilizes the engine speed. The flywheel can also have crank pins that indicate the engine position, but in the engines equipped with EMS the engine position is detected by cam and crankshaft position sensors as explained above.



Figure 4-24: Wärtsilä 34SG engine. By courtesy of Wärtsilä [28][4]

It is important that the delays of the signals from the engine position sensors are kept low. The maximum delay depends on the type of engine. The crank and cam signals are galvanically separated from the rest of the system to eliminate interference. The sensors used for the crank and cam signals have limited driving power and the signals are therefore buffered in the KM. Each KM can supply the crank and cam signals to up to 6 CM units. The maximum engine speed is 1800 rpm and the maximum frequency of the crank position pulse train signal is

$$f = \frac{n \cdot \text{crank}}{2 \cdot 60} = \frac{1800 \cdot 900}{2 \cdot 60} = 13.5 \text{ kHz} \Rightarrow T = \frac{1}{13.5\text{k}} = 74 \mu\text{s} \quad (22)$$

where n is the engine speed in rpm and crank is the number of pulses per two engine revolutions.

900 pulses per two engine revolutions and a frequency of 13.5 kHz yields a 74 μs period time for the crank signal. This is important for the allowed rise- and fall times of the electronics.

The delay of the boosted crank signal can be maximum 9.3 μs when a tolerance of 0.1 degrees is accepted according to

$$t_{\max \text{ delay}} = \frac{1}{\frac{n}{60} \cdot 360} \cdot \text{tolerance} = \frac{1}{\frac{1800}{60} \cdot 360} \cdot 0.1 = 9.3 \mu\text{s} \quad (23)$$

where n is the engine speed in rpm and tolerance is the maximum accepted delay in degrees of the crank signal. However, the known delay, rise- and fall times can be compensated for in the microcontroller when calculating the engine position. It is the variation in the threshold voltages in the Schmitt trigger that will cause most of the error in the engine position signals that cannot be compensated for.

The crank and cam signals are connected to a high speed optocoupler, HCPL-0600 [29] and the signals are buffered with a transistor, Si4948, see Figure 4-28. The operational amplifier LM258 [30] and the comparator LM2901 [31] are used to protect the crank and cam outputs in case of short circuit connection.

A differential amplifier is used in the current protection circuit, see Figure 4-25. The differential amplifier output is connected to a Schmitt trigger with hysteresis, see Figure 4-26 and when the current becomes too high the Schmitt trigger output will change status and the current will be turned off, see Figure 4-28.

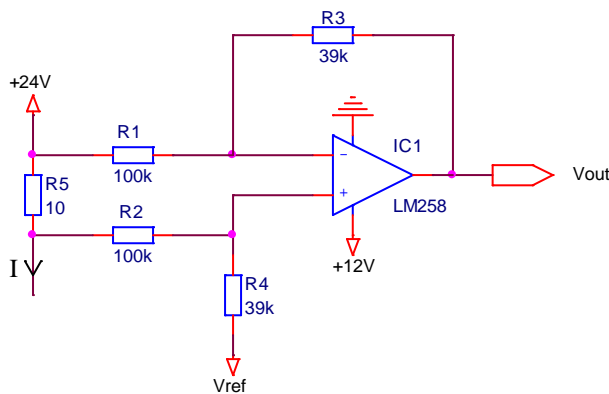


Figure 4-25: Differential amplifier as a current sensor

The output voltage when $R_1 = R_2$, $R_3 = R_4$ and $R_1 \gg R_5$ is

$$V_{out} = V_{ref} + R_5 \cdot I \cdot \frac{R_3}{R_1} \quad (24)$$

The leakage currents can be neglected when R_1 and R_2 are much larger than R_5 .

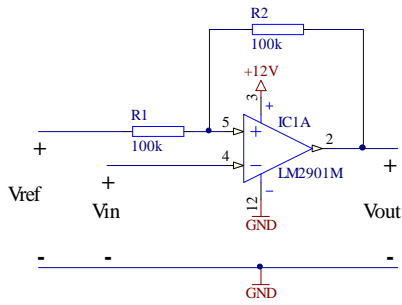


Figure 4-26: Schmitt trigger with variable hysteresis

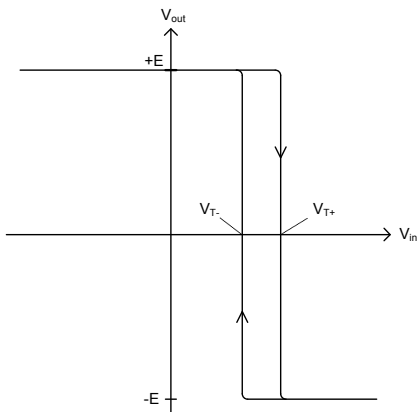


Figure 4-27: Schmitt trigger hysteresis

The threshold voltages in Figure 4-27 are

$$V_{T+} = +E \cdot \frac{R_2}{R_1 + R_2} + V_{ref} \cdot \frac{R_1}{R_1 + R_2} \quad (25)$$

$$V_{T-} = -E \cdot \frac{R_2}{R_1 + R_2} + V_{ref} \cdot \frac{R_1}{R_1 + R_2} \quad (26)$$

where +E is the positive supply voltage and -E is the negative supply voltage.

Figure 4-28 shows the schematic of the engine position circuit. The engine position signals are protected from damage from a short circuit connection by a current sensing resistor. When the outputs are shorted the current through the current sensing resistor increases and so does the voltage across the resistor and the differential amplifier output voltage. The comparator turns the transistor off when the threshold current is reached and the current goes to zero.

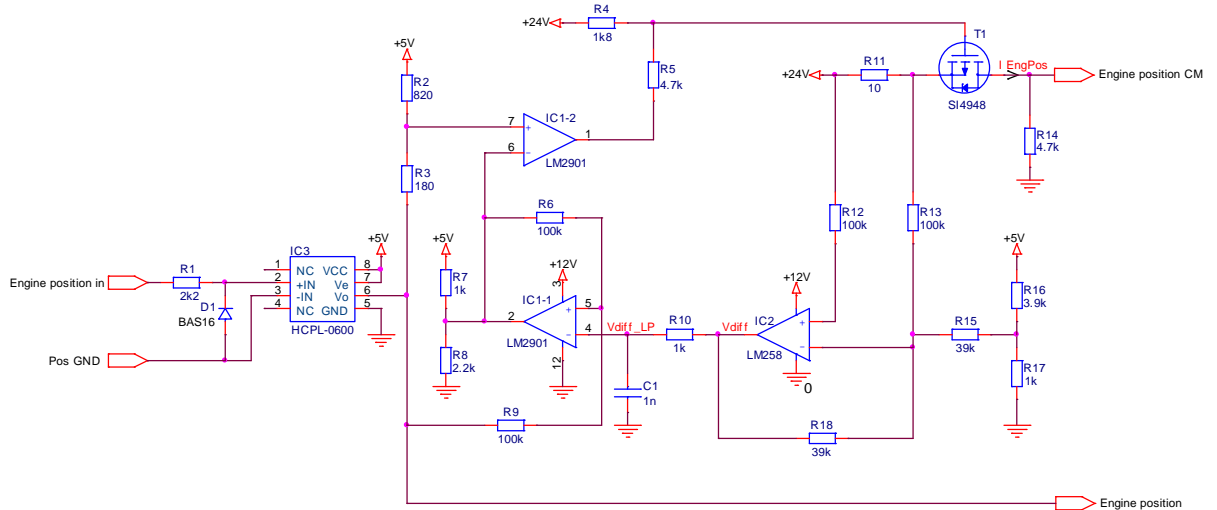


Figure 4-28: Schematic of the KM engine position signals

Using equations (25) and (26) for the schematic in Figure 4-28 yields for a single supply voltage and open collector output of the LM2901 comparator

$$\begin{aligned}
 V_{T+off} &= +E \cdot \frac{R_9}{R_9 + R_6} + V_{EngPos} \cdot \frac{R_6}{R_9 + R_6} = \\
 &= \frac{2.2}{2.2 + 1} \cdot 5 \cdot \frac{100}{100 + 100} + 0 \cdot \frac{100}{100 + 100} = 1.7 \text{ V}
 \end{aligned} \tag{27}$$

when the engine position signal is low and

$$\begin{aligned}
 V_{T+on} &= +E \cdot \frac{R_9}{R_9 + R_6} + V_{EngPos} \cdot \frac{R_6}{R_9 + R_6} = \\
 &= \frac{2.2}{2.2 + 1} \cdot 5 \cdot \frac{100}{100 + 100} + 5 \cdot \frac{100}{100 + 100} = 4.2 \text{ V}
 \end{aligned} \tag{28}$$

when the engine position signal is high.

$$V_{T-off} = V_{EngPos} \cdot \frac{R_9}{R_9 + R_6} = 0 \cdot \frac{100}{100 + 100} = 0 \text{ V} \tag{29}$$

when the engine position signal is low and

$$V_{T-on} = V_{EngPos} \cdot \frac{R_9}{R_9 + R_6} = .5 \cdot \frac{100}{100 + 100} = 2.5 \text{ V} \tag{30}$$

when the engine position signal is high.

The turn off voltage when the engine position is high is 1.7 V according to equation (27) and the maximum current, see schematic in Figure 4-28 and simulation in Figure 4-30, is therefore, using equation (24)

$$I_{EngPosmax} = \frac{V_{diff} - \frac{R_{I7}}{R_{I7} \cdot R_{I6}} \cdot 5}{\frac{R_5 \cdot R_{I8}}{R_{I2}}} = \frac{1.7 - \frac{1000}{10000} \cdot 5}{\frac{10 \cdot 39000}{100000}} = 0.17 \text{ A} \quad (31)$$

The maximum current when 6 CM units are connected to the KM is

$$I_{EngPos} = \frac{29}{\frac{4.7}{7}} = 43 \text{ mA} \quad (32)$$

which yields an output voltage using equation (24) from the differential amplifier of

$$V_{diff} = \frac{1}{3.9 + 1} \cdot 5 + 10 \cdot 0.043 \cdot \frac{39}{100} = 1.2 \text{ V} \quad (33)$$

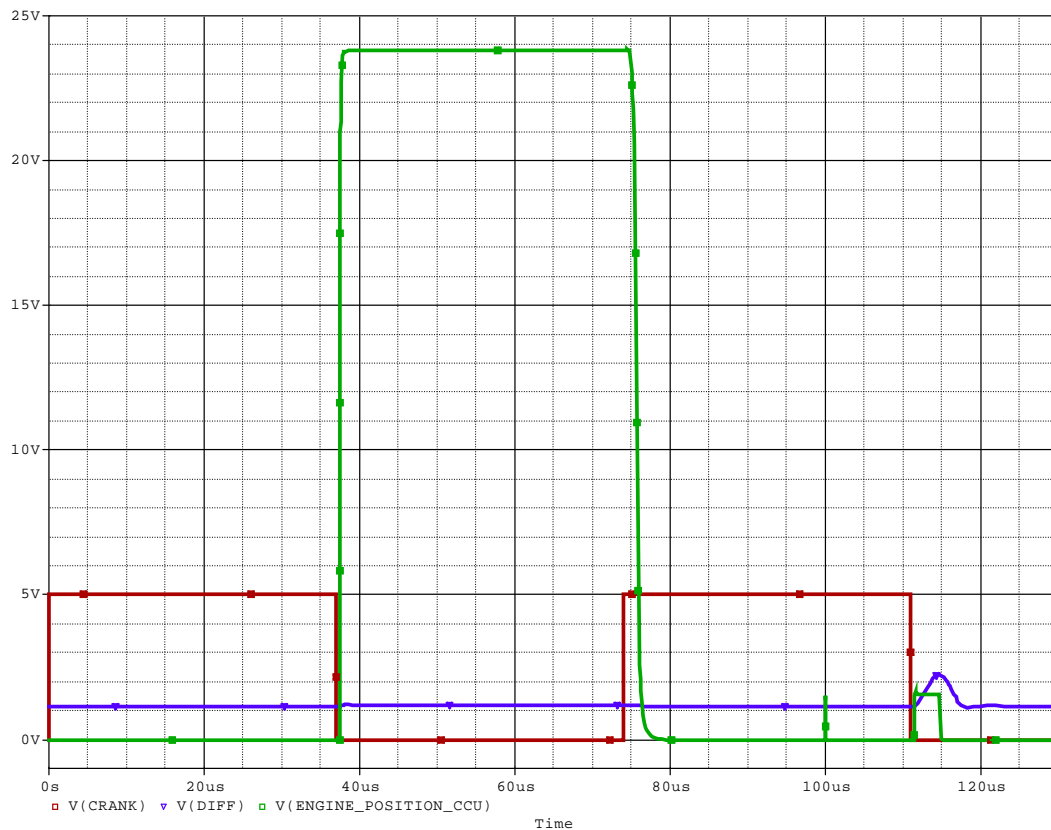


Figure 4-29: Boost of the crank and cam signals in the KM to the CM and the effect of the protection from short circuit connection. The inverted crank signal from the sensors is red, the buffered crank signal is green and the differential amplifier output is blue.

The engine position signal is shorted to ground after 100 μs , see Figure 4-29 and that is why the output voltage decreases to zero volts after about 115 μs . The transistor is turned off and the output voltage and current goes to zero. The simulation also shows

that there is almost no delay at turn on and a delay of almost 5 μs at turn off which is less than 0.1 degrees according to equation (23).

Figure 4-30 shows a simulation of the effects of a too high position current. This happens when the engine position signals are shorted. The transistor is turned off when the voltage drop over the current sense resistor exceeds 1.7 V after 41 μs . The simulation result agrees well with the calculated result, equation (31).

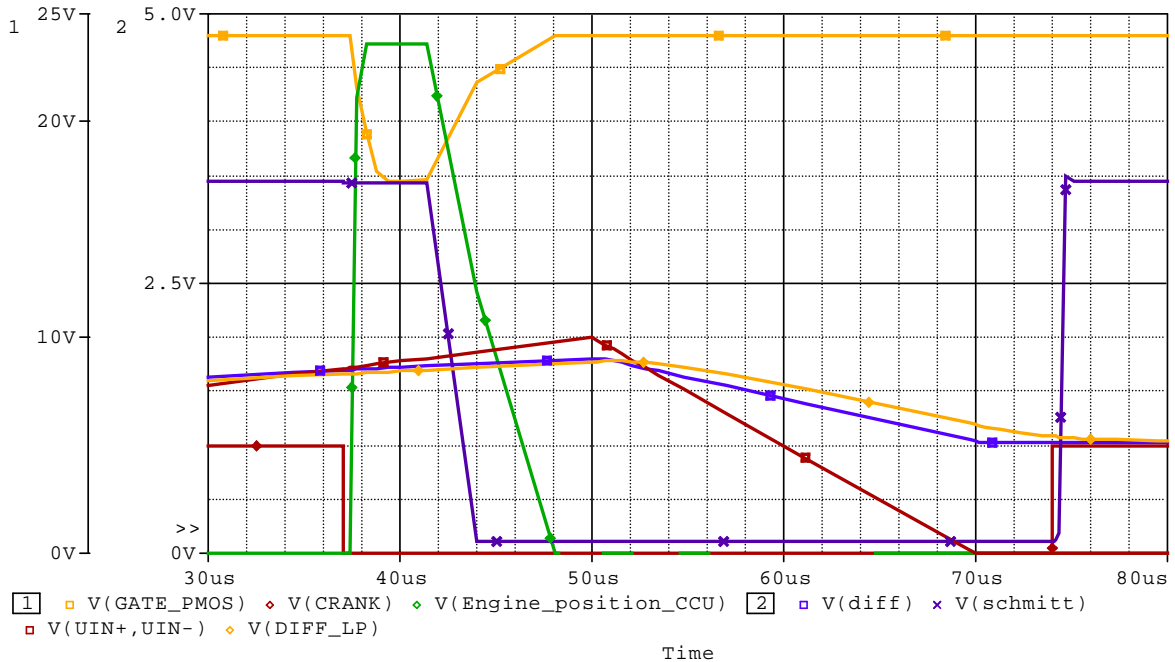


Figure 4-30: Simulation of the protection from short circuit connection of the engine position circuit. The engine position (crank) signal is red / diamond, the gate voltage of the transistor is orange / square, the engine position output voltage to the CM is green / diamond, the voltage drop over the current sense resistor is red / squares, the output voltage from the Schmitt trigger is purple / x, the differential amplifier output voltage is blue / squares and orange / diamonds after the LP filter

Figure 4-31 shows the schematic of the circuit for the CM engine position signals. A general purpose photocoupler PC357N [32] is used to galvanically isolate the engine position signals. The Schmitt trigger 74HC14 [33] creates a square wave engine position signal that is connected to the eTPU2 in the microcontroller. The crank and cam signals to the CM are the buffered engine position signals from the KM, see Figure 4-28.

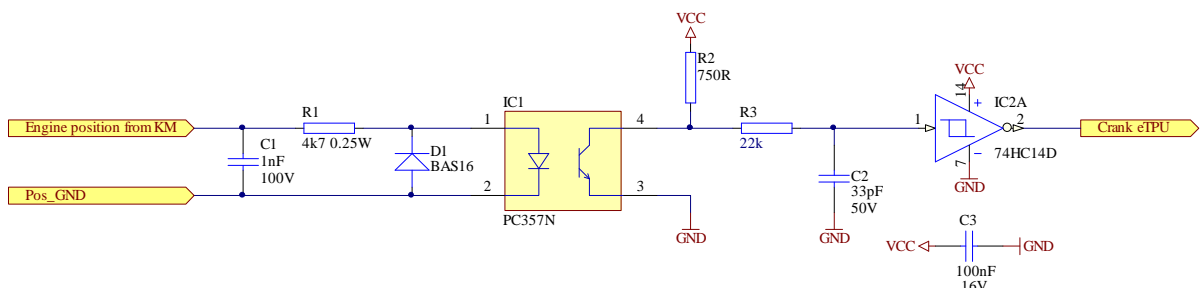


Figure 4-31: Schematic of the CM engine position signals (crank and cam signals)

The schematics in Figure 4-28 and Figure 4-31 yield a minimum current to the photocoupler in Figure 4-31 of

$$I_{F\min} = \frac{V}{R} = \frac{19}{4.7} = 4 \text{ mA} \quad (34)$$

The minimum current transfer ratio (CTR) for PC357N is $200\% \cdot 0.7 = 140\%$ at $+85^\circ\text{C}$ ambient temperature [32] and the minimum collector current is

$$I_{C\min} = CTR \cdot I_F = 1.4 \cdot 4 = 5.6 \text{ mA} \quad (35)$$

which yields a maximum V_{CE} with a 750Ω load resistor

$$V_{ce\max} = V_{CC} - R_L \cdot I_C = 5 - 0.75 \cdot 5.6 = 0.8 \text{ V} \quad (36)$$

The minimum negative-going threshold (V_T) is 1 V for 74HC14 [33] and therefore the maximum allowed collector-emitter voltage (V_{CE}) for the photocoupler PC357N is [32] also 1 V. The minimum load resistor is therefore

$$R_{\min} = \frac{V_{CC} - V_{CE\min}}{I_{C\min}} = \frac{5 - 1}{5.6\text{m}} = 714 \Omega \quad (37)$$

The rise and fall times increase when the load resistance increases and the resistance should therefore be chosen as low as possible. The response time for PC357N [32] is only given in the datasheet for a collector current of 2 mA. The rise- (t_r) and fall times (t_f) are about $17 \mu\text{s}$ respectively and the propagation delay from high to low, t_d is about $3 \mu\text{s}$ and the propagation delay from low to high, t_s is $1 \mu\text{s}$, see Figure 4-32. The engine position signals are therefore delayed by a maximum of $20 \mu\text{s}$ which is just over 0.2 degrees, see equation (23). The rise- and fall times are between 10% and 90% of the signal voltage range.

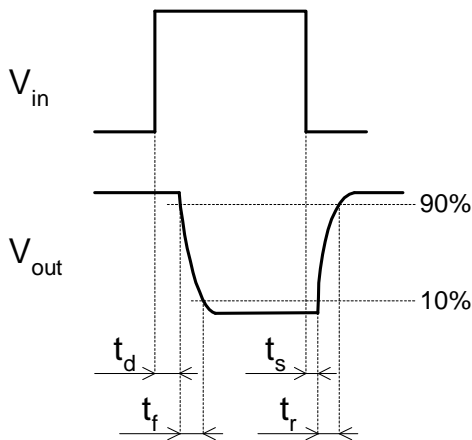


Figure 4-32: Definition of time response for PC357

The definitions of the threshold voltage and hysteresis are shown in Figure 4-33.

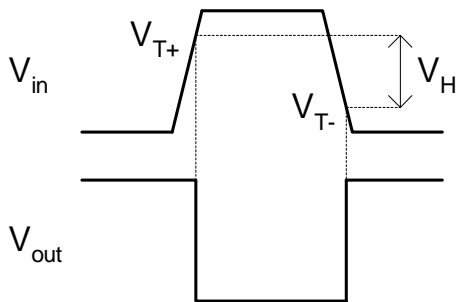


Figure 4-33: Definitions of V_{T+} , V_{T-} and V_H

The engine position signal is measured on rising edges causes. The spread of the negative-going threshold in the Schmitt trigger causes the error in the engine position signals. The minimum V_{T-} is 1.9 V and the maximum is 2.2 V which causes an approximate error that cannot be compensated of

$$t_{error} = \frac{17}{4.5 - 0.5} \cdot (2.2 - 1) = 5.1 \mu s \quad (38)$$

which is less than 0.1 degrees, see equation (23).

There are buffers and operational amplifier circuits protected from short circuit connection and thermal shut down but unfortunately it was impossible to find one that satisfies the voltage, speed, current and temperature requirements in the EMS specification. The input voltage range is not good enough for the operational amplifier OPA551 [34] and the buffer EL2001C [35] does not satisfy the temperature range requirements. These are two examples from a number of buffers and operational amplifier circuits that have been analyzed.

4.8 Knock - KM

Piezoelectric vibration sensors are used to detect knock. In the EMS face lift a lot of the hardware used for detecting knock has been replaced by software. The filtering and signal processing are examples of functions that are now implemented in software instead of in hardware.

Knock detection and diagnosis are performed on the signals from the sensors. Knock detection is to detect knock and diagnosis is for controlling that the sensor is working properly. There is only one signal and the knock detection and diagnosis are performed on different engine positions with different timeframes.

The signals from the piezoelectric vibration sensors are differential with a floating potential. The sensors are therefore connected to differential amplifiers, see Figure 4-34 which adapt the signals to the microcontroller level of maximum 5 V. A single supply

rail-to-rail precision operational amplifier with low offset voltage and low input bias current is needed for the differential amplifier, for instance OP491 [36] or AD8608 [37]. A single supply voltage of 5 V and a reference voltage of half the supply voltage are used. The output signal is centered on the reference voltage and the maximum output swing is ± 2.5 V. The output signal is connected to the AD converter in the microcontroller for signal processing. The microcontroller band pass filters the signal and checks if the engine is knocking during the knock detection windows and that the knock sensors are operating properly during the diagnosis windows.

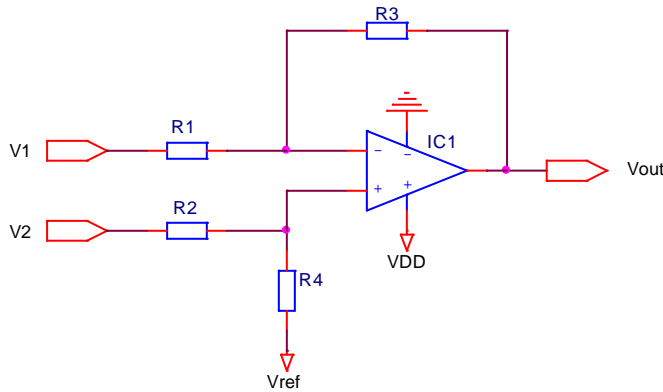


Figure 4-34: Differential amplifier for the knock signal

The output voltage when $R_1 = R_2$ and $R_3 = R_4$ is

$$V_{out} = V_{ref} + (V_2 - V_1) \cdot \frac{R_3}{R_1}, \quad 0 < V_{out} < VDD \quad (39)$$

It is important to match the resistors in the differential amplifiers if there is a common mode voltage on the input signals and therefore 0.1% precision resistors are used.

4.9 Power Supply

The main power supply voltage to the CM and KM can vary between 19 and 29 V and the CM and KM must be protected from reverse battery connection. The main and PCC injectors in the CM are connected to the available supply voltage, the injector driver circuits use +12 V and the microcontroller uses a +5 V supply voltage.

The main supply voltage in the CM drives the injectors, see Figure 4-35. It is stabilized and rectified with a large electrolytic capacitor, a transil, a diode and some ceramic capacitors. A +12V supply voltage is also used in the CM as a backup voltage for the logic components if the main power supply is disconnected.

The KM power supply, see Figure 4-36, is similar to the CM. The main difference is due to the fact that the KM has less current consumption and therefore there is no need for the large electrolytic capacitor. The +12 V supply voltage is only used for the low power operational amplifiers and comparators. The 100 mA MC78L12A voltage regulator is used to create this voltage.

Both the CM and the KM have an adjustable step down switching regulator LM2576 [39] that is used to create a 6 V signal and that signal is converted to 5 V by a low drop linear voltage regulator LP3962 [40] with an error signal that can be used as a reset signal to the microcontroller. The step down switching regulator has higher efficiency than a linear regulator and no heat sink is necessary. Therefore this is used when the +24 V supply voltage is converted to 6 V voltage. The linear regulator is more accurate and does not need a heat sink when the input voltage is just 1 volt higher than the output voltage so a high accuracy linear regulator is used to convert the 6 V voltage to 5 V. A voltage regulator MC7812 [41] in the CM is used to supply the injector drivers with +12 V.

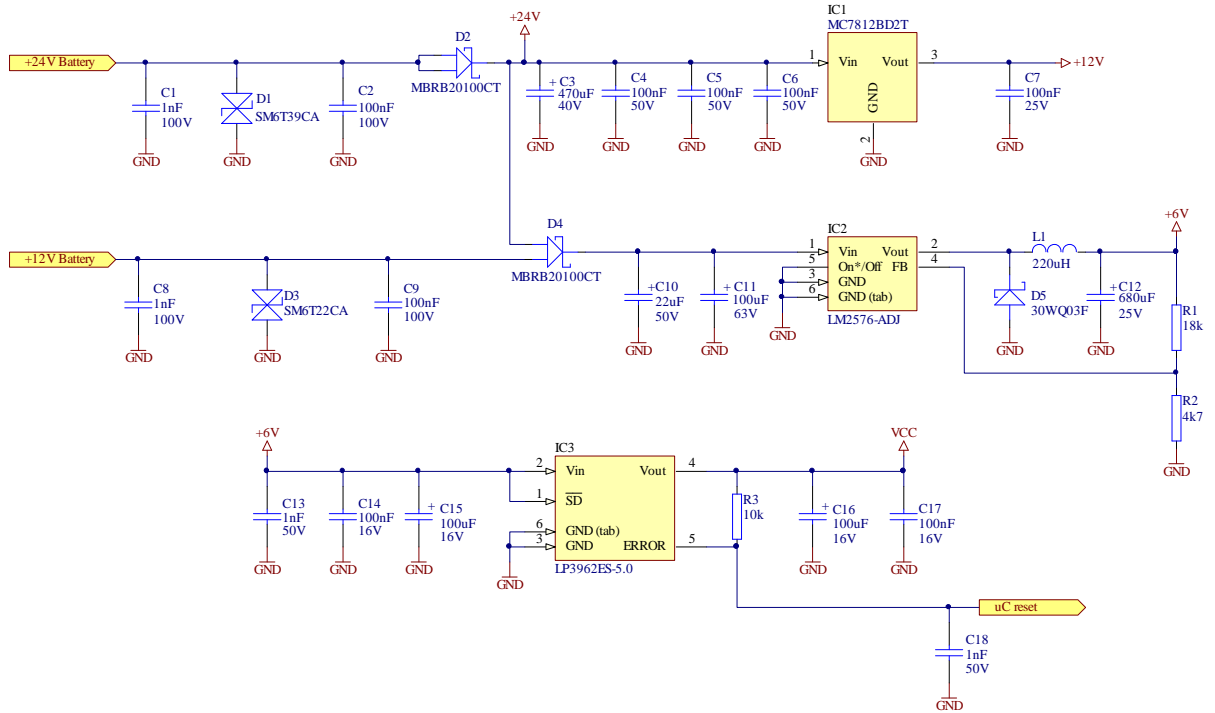


Figure 4-35: CM power supply schematic

The resistances R1 and R2 in Figure 4-35 are used to program the output voltage according to [39]

$$V_{out} = V_{ref} \cdot \left(1 + \frac{R_1}{R_2} \right) \quad \text{where } V_{ref} = 1.23 \text{ V and } 1 \text{ k}\Omega \leq R_2 \leq 5 \text{ k}\Omega \quad (40)$$

R₂ is chosen to 4.7 kΩ which gives R₂ = 18.2 kΩ. The closest value in the E24 series is 18 kΩ and with 1% tolerance on the resistors and ±4% tolerance on the output voltage for the adjustable LM2576 [39] the minimum output voltage is 5.61 V. The absolute maximum voltage drop for LP3962 [40] is 550 mV and therefore the chosen resistor values are acceptable.

The value of the inductor L1 in Figure 4-35 is chosen by calculating the inductor Volt · microsecond constant ($E \cdot T$ [V · μ s]) [39]

$$E \cdot T = (V_{in} - V_{out}) \cdot \left(\frac{V_{out}}{V_{in}} \cdot \frac{1000}{f} \right) \quad (41)$$

where f is given in kHz and $f = 52$ kHz for LM2576, V_{in} and V_{out} input and output voltage respectively. The $E \cdot T$ value is then used in the “Inductor Value Selection Guide” diagram in the datasheet [39]. An input voltage of 19 – 29 V yields $E \cdot T = 79$ V · μ s and $E \cdot T = 92$ V · μ s respectively. A maximum current of 1.3 A gives a L220 inductor and the Pulse PE-52626 is chosen. The catch diode, D8 in Figure 4-35, is selected to 30WQ03F according to the “Diode Selection Guide” in the ON LM2576 datasheet [42]. The input and output capacitors are chosen to 100 μ F and 680 μ F according to “LM2576 Series Buck Regulator Design Procedure” in the National datasheet [39].

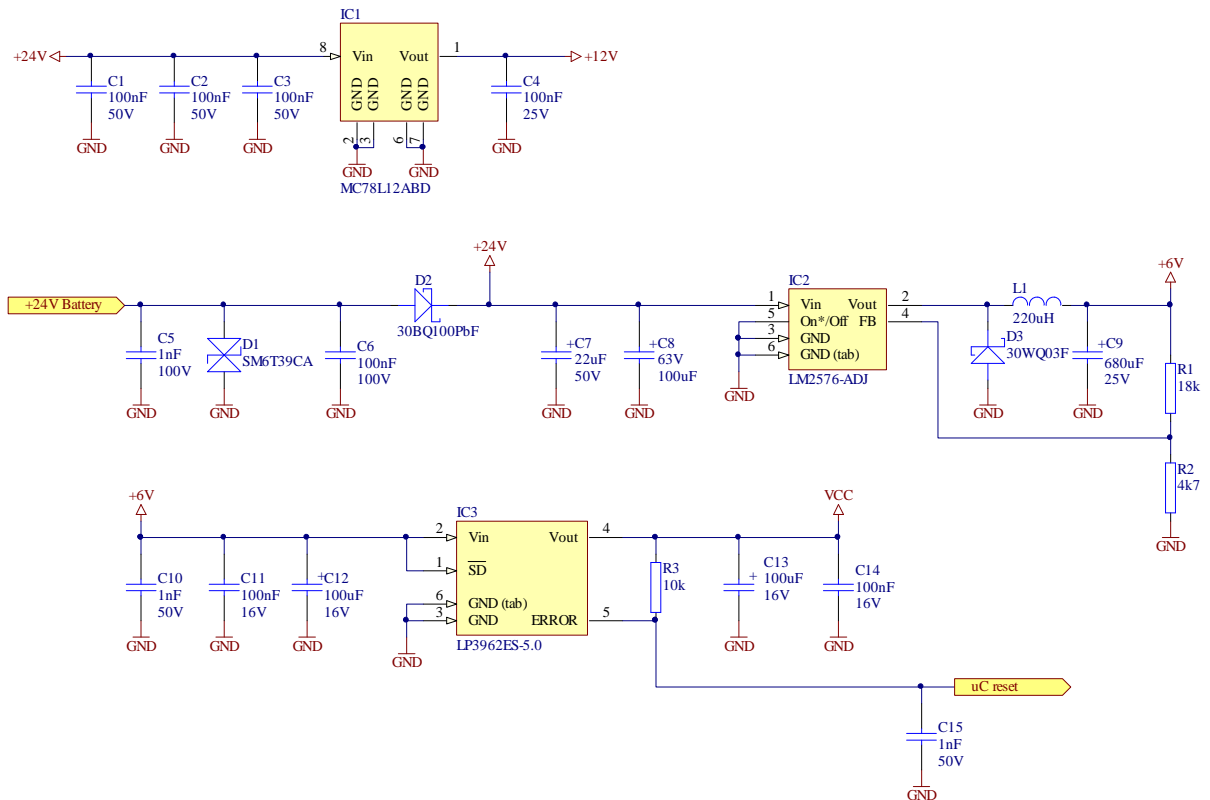


Figure 4-36: KM power supply schematic

A green LED controlled by the microcontroller indicates that the power supply to the microcontroller is working correctly, see Figure 4-37.

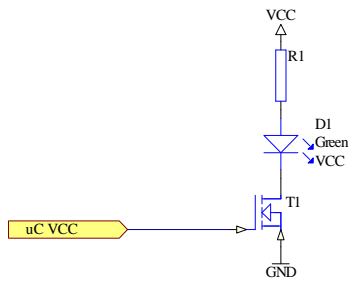


Figure 4-37: Schematic of the indication with a LED of correct power supply to the microcontroller

4.10 Printed Circuit Board

There are several different software programs for drawing a schematic and designing a printed circuit board (PCB). Mentor, OrCAD and Altium Designer are some of the most used programs. In this project, Altium Designer was used.

4.10.1 Design Rules

There are many rules to consider when designing a PCB. The following must be considered

- The mechanical dimensions of the PCB and mounting method
- Connections to the PCB
- Decoupling of all interference signals and connections to the PCB
- How the circuit can be partitioned. Analog circuits, radio frequency signals, digital subsystems and power stages must be kept separate
- How critical paths can be keep as short as possible
- Design of footprints according to the mounting and soldering process
- Minimum distances between different parts of the PCB
- The width of the tracks
- Use of ground and power planes
- EMC

The first thing that needs to be done when designing a PCB is to determine all mechanical limitations in all three dimensions and how the PCB will be fastened. With this information the mechanical layer and all fastening holes, if any, can be drawn. The second step is to decide how the input and output signals will be connected to the PCB. If a contact is to be used, its footprint is then placed on the layout.

When all the mechanical details are determined the actual layout work can begin. All interference signals must be decoupled so other signals will not be affected. Low level analog circuits, radio frequency signals, digital subsystems and power stages should be kept separate as far as possible to avoid interference. Critical paths should be kept as short as possible. The minimum distance between components and between tracks depends on for instance the mounting and soldering method and the method used by the PCB manufacturer. When reflow soldering is used for all surface mounted components and selective soldering for all lead components the distance between the pads for the lead components and the surface mounted component must be increased compared to when manual soldering of the lead components is used. Wave soldering cannot be used for fine pitch packages and balled grid arrays (BGA) packages.

The minimum isolation distance depends on the voltage differences between the different nets [43]. The minimum width of the track depends on the PCB material, the current in the track and the allowed temperature rise in the track [44].

The most common material in PCBs is FR-4, made of woven glass and epoxy. There are several versions of FR-4, the main difference is the type of epoxy that is used. There are also different dielectrics that can be chosen to provide different insulating values depending on the requirements of the circuit. Conducting layers are typically made of thin copper foil. The copper is usually 18 μm , 35 μm or 70 μm thick. The board is typically coated with a green solder mask to increase the isolation and protect the copper.

4.10.2 PCB Design

The current CM and KM have two PCBs each. The I/O board is mounted at the bottom of the casing and the CPU board is mounted in the lid. The boards are connected by flat conductor cables. All contacts cause an increased risk for mechanical problems. Therefore the redesign will if possible only use one PCB in the CM and one PCB in the KM. The PCBs will be mounted at the bottom of the casings where the I/O board is mounted in the current system. The PCBs is fastened by six screws each.

The distance from the bottom of the casing to the PCB is 3.2 mm in the current system. Some of the power components are mounted against the casing to lower the junction temperature. All power components are surface mounted in the redesign and will therefore not be mounted against the casing. However, some of the surface mounted power components are higher than 3.2 mm and the distance from the PCB to the bottom of the casing must therefore be increased. The D²PAK case and TO-263 case are the highest surface mounted components used in the redesign, the height is maximum 4.65 mm for those cases. 4856 force-fit standoffs or 5059-2 swage spacers from Keystone [45] can be used to raise the board from the bottom of the casing.

The contacts for all the in- and output signals to the CM and KM are spring-cage connectors. Spring-cage connection has better resistance to vibrations than screw connection. The Phoenix contact ZFKDS 2.5 [46] is used in this design.

4.11 Reliability Prediction of Electronic Equipment

MIL-HDKB-217F is a military handbook for reliability prediction of electronic equipment [47], [48]. It is a standardization handbook that was developed by the Department of Defense with assistance of the military departments, federal agencies and industry for reliability prediction of electronic equipment. MIL-HDKB-217F is for guidance only and should not be cited as a requirement.

The failure rate model for a mated pair one pin connectors is [48]

$$\lambda_p = \lambda_b \cdot \pi_T \cdot \pi_K \cdot \pi_Q \cdot \pi_E \text{ failures / } 10^6 \text{ hours} \quad (42)$$

where λ_b is the base failure rate, π_T is the temperature factor, π_K is the mating/unmating factor, π_Q is the quality factor and π_E is the environmental factor.

Using equation (42) for a one pin mated pair PCB connector used in EMS yields

$$\lambda_p = \lambda_b \cdot \pi_T \cdot \pi_K \cdot \pi_Q \cdot \pi_E = 0.040 \cdot 2.5 \cdot 1 \cdot 1 = 0.2 \text{ failures / } 10^6 \text{ hours} \quad (43)$$

which yields 5.6 failures / 10^6 hours for two mated pair 14 pin connectors used in the old EMS to connect the two boards.

The failure rate model for a resistor is [48]

$$\lambda_p = \lambda_b \cdot \pi_T \cdot \pi_P \cdot \pi_S \cdot \pi_Q \cdot \pi_E \text{ failures / } 10^6 \text{ hours} \quad (44)$$

where λ_b is the base failure rate, π_T is the temperature factor, π_P is the power factor, π_S is the power stress factor, π_Q is the quality factor and π_E is the environmental factor.

Using equation (44) for a 0603 size resistor with 0.1 W power rating used in EMS yields

$$\lambda_p = \lambda_b \cdot \pi_T \cdot \pi_P \cdot \pi_S \cdot \pi_Q \cdot \pi_E = 0.0037 \cdot 1.69 \cdot 0.31 \cdot 1.23 \cdot 10 \cdot 4 = 0.095 \quad (45)$$

failures / 10^6 hours for a resistor with 0.05 W power dissipation and

$$\lambda_p = \lambda_b \cdot \pi_T \cdot \pi_P \cdot \pi_S \cdot \pi_Q \cdot \pi_E = 0.0037 \cdot 1.69 \cdot 0.31 \cdot 0.79 \cdot 10 \cdot 4 = 0.061 \quad (46)$$

failures / 10^6 hours for a resistor with 0.01 W power dissipation.

The failure rate model for a capacitor is [48]

$$\lambda_p = \lambda_b \cdot \pi_T \cdot \pi_C \cdot \pi_V \cdot \pi_{SR} \cdot \pi_Q \cdot \pi_E \text{ failures / } 10^6 \text{ hours} \quad (47)$$

where λ_b is the base failure rate, π_T is the temperature factor, π_C is the capacitance factor, π_V is the voltage stress factor, π_{SR} is the series resistance factor (for tantalum CSR style capacitors only), π_Q is the quality factor and π_E is the environmental factor.

Using equation (47) for a 100 nF / 25 V ceramic capacitor used in EMS yields

$$\lambda_P = \lambda_b \cdot \pi_T \cdot \pi_C \cdot \pi_V \cdot \pi_{SR} \cdot \pi_Q \cdot \pi_E = 0.00099 \cdot 9.82 \cdot 0.89 \cdot 1.0 \cdot 3 \cdot 10 = 0.26 \quad (48)$$

failures / 10^6 hours when the operating voltage is 5 V.

The 680 μ F / 25 V electrolytic aluminum oxide capacitor used in EMS, see Figure 4-35 and Figure 4-36, yields

$$\lambda_P = \lambda_b \cdot \pi_T \cdot \pi_C \cdot \pi_V \cdot \pi_{SR} \cdot \pi_Q \cdot \pi_E = 0.00012 \cdot 9.82 \cdot 4.48 \cdot 1.01 \cdot 10 \cdot 10 = 0.53 \quad (49)$$

failures / 10^6 hours when the operating voltage is 6 V.

The 100 μ F / 63 V electrolytic aluminum oxide capacitor used in EMS, see Figure 4-35 and Figure 4-36, yields

$$\lambda_P = \lambda_b \cdot \pi_T \cdot \pi_C \cdot \pi_V \cdot \pi_{SR} \cdot \pi_Q \cdot \pi_E = 0.00012 \cdot 9.82 \cdot 2.88 \cdot 1.26 \cdot 10 \cdot 10 = 0.43 \quad (50)$$

failures / 10^6 hours when the operating voltage is 29 V.

Equations (42) – (50) indicate that connectors have great impact on the failure rate and that electrolytic capacitors also have a high failure rate.

Corresponding calculations may be done on all components in the system. Adding those results and then inverting the result yields the system Mean Time Between Failure (MTBF).

Removing the connectors that connect the two boards in the old design and using fewer components in the new system increases the MTBF for the system.

5 Result

The redesign of the CM and KM resulted in an increased mechanical reliability mainly because

- There is only one PCB in each unit and therefore no flat conductor cables with connectors as in the current design
- Spring-cage connectors are used instead of screw-cage connectors
- Only surface mounted power components are used and therefore no components need to be mechanically attached to the casing for cooling

All of the components used in the redesign are recommended for new designs. No obsolete or components that are not recommended for new designs are used.

The number of components has been reduced from 441 components in the old CM system to 245 components in the new design and from 393 components in KM to 211 components.

The injector driver is improved in the new design. The injector driver in the new design is, unlike the old design, protected from short circuit connections.

6 Discussion

All components used in the redesign are recommended for new designs. Therefore the redesign of the EMS should make it possible to produce the system as long as there are engines using the system and spare parts are needed. This time is maybe 15 – 20 years and some of the components in the current system will not be in production that long. The microcontroller that is used is one of those components, it will probably only be in production for another 5 – 10 years.

The main differences between the current system and the redesign are that some of the functions that are implemented in hardware in the current system will now be implemented in software, that only components recommended for new design have been used and that there is only one PCB in each unit instead of two. One PCB increases the mechanical reliability and the microcontroller used is very powerful.

Other reasons that the design only needs one PCB in each unit are that all external AD converters and memories no longer are needed since the microcontroller has internal AD converters and sufficient internal memory.

Connectors have a much high failure rate than other components although those too may fail [47], [48]. By removing the connectors between the two boards in the old system and by reducing the number of components to almost half, the failure rate for the system has been reduced.

The eTPU2 can be programmed separately and there should therefore be no problems with timing when controlling the injector currents in the CM.

The main difference in the KM is that the external filter components are removed and the software is used to filter the signals instead.

Since the mechanical design of the casing must not be changed spacers must be mounted on the PCB to increase the distance from the bottom of the casing to the PCB. In this way the old system can easily be replaced when needed by the redesigned system as the casings are identical.

The software has not yet been developed for the new design. It is therefore not possible to build a prototype and verify the EMS facelift design. This software falls outside the scope of this project.

7 Terminology

Table 7.1: Terminology

Acronym	Definition
ADC	Analog-to-Digital Converter
BAM	Boot Assist Module
CAN	Controller Area Network
CM	Cylinder Module
CND	Compressed Natural Gas
CNG	Compressed Natural Gas
CPU	Central Processing Unit
CRD	Customer Requirement Documentation
CTR	Current Transfer Ratio
EMS	Engine Management System for Natural Gas
ESR	Equivalent Series Resistance
DMA	Direct Memory Access
DSP	Digital Signal Processor / Processing
EMC	ElectroMagnetic Compatibility
eMIOS	Enhanced Modular Input-Output System
eQADC	Enhanced Queued Analog-to-Digital Converter
eTPU	Enhanced Time Processor Unit
FIR	Finite Impulse Response
GPIO	General Purpose Input Output
HCO	Hoerbiger Control Systems
HSD	High Side Driver
IIR	Infinite Impulse Response
I/O	Input / Output
JTAG	Joint Test Action Group
KM	Knock Module
LQFP	Low Profile Quad Flat Package
LSD	Low Side Driver
Main CC	Main Combustion Chamber
MC	Master Controller
MS	Module Specification
MTBF	Mean Time Between Failure
PBGA	Plastic Ball Grid Array
PCB	Printed Circuit Board
PCC	Pre-Combustion Chamber
QHB	Quality Handbook
QT	Quote
RAM	Random Access Memory
RS	Requirement Specification
SCI	Serial Communication Interface
SPI	Serial Peripheral Interface
SS	System Specification
TC	Thermocouple
TDC	Top Dead Center

8 References

- [1] Wärtsilä (2009). *Wärtsilä gas & dual / tri-fuel engines*. [www]. <<http://www.wartsila.com/.en.productservices.productportfolio.product..32105987216222770.no.8003.htm?cid=HF003>>. 2009-04-29.
- [2] Wärtsilä (2009). *Wärtsilä Products*. [www]. <<http://www.wartsila.com/.en.productservices.productportfolio.product..3611923571543040.no.8000.htm>>. 2009-04-29.
- [3] Martin.G.M. & Hattar. C. (2008). *The Wärtsilä 34SG engine as a cost-effective compressor drive*. [www]. <http://www.wartsila.com/Wartsila/global/docs/en/about_us/in_detail/1_2008/cost-effective-compressor-drive-wartsila34sg.pdf>. 2009-04-29.
- [4] Wärtsilä Legal and Privacy notice. *Legal and Privacy notice*. [www]. <<http://www.wartsila.com/.en.investors.0.legalnotice.C618967A-055E-4E60-BD48-CECA797D558F.1BDBC0D2-812B-4199-8C12-0027BDD37F99...htm>>. 2009-04-29.
- [5] Moore. Gordon E. Cramming more components onto integrated circuits. *Electronics*. 19 April 1965.
- [6] MPC5632 Freescale Microcontroller. *MPC563XM Microcontroller Reference Manual*. [www]. <http://www.freescale.com/files/32bit/doc/ref_manual/MPC563XMRM.pdf?fsrch=1> Rev. 1. 25 Jul 2008
- [7] MPC5632 Freescale Microcontroller. *MPC5534 Microcontroller Data Sheet*. [www]. <http://www.freescale.com/files/32bit/doc/data_sheet/MPC5534.pdf?fsrch=1> Rev. 4.0. 25 March 2008
- [8] *MPC5534 Microcontroller Reference Manual*. [www]. <http://www.freescale.com/files/32bit/doc/ref_manual/MPC5534RM.pdf?fsrch=1>. Rev. 2 5 Oct 2008.
- [9] BCP68T1 ON Semiconductor datasheet. *BCP68T1 NPN Silicon Epitaxial Transistor*. [www]. <http://www.onsemi.com/pub_link/Collateral/BCP68T1-D.PDF>. October. 2005 – Rev. 5
- [10] 92SM crystal. *SMI Quartz Crystal Units 92SMX FAMILY STANDARD SMD CRYSTALS*. [www]. <http://www.smi-xtal.com/product/pdf/92SMX_FAMILY.pdf>.
- [11] 94HBB10 binary rotary switch. *Grayhill Rotary DIP Switches SERIES 94H Binary Coded*. [www]. <http://www.grayhill.com/catalog/DIP_Series_94H.pdf>.
- [12] *Woodward SOGAV 43. 105. & Balanced 105 Solenoid Operated Gas Admission Valve*. [www]. <<http://www.woodward.com/pdf/ic/04151.pdf>> 04151 (Rev. L).
- [13] *Woodward SOGAV 2.2 Solenoid Operated Gas Admission Valve*. [www]. <<http://www.woodward.com/pdf/ic/04172.pdf>> 04172 (Rev. G).
- [14] IPB05CN10N G Infineon datasheet. *Infineon OptiMOS 2 Power-Transistor*. [www]. <http://www.infineon.com/dgdl/IPP05CN10N_Rev1.07.pdf?folderId=db3a3043156fd5730115c7d50620107c&fileId=db3a3043156fd5730115c7e3e68a108d> Rev. 1.05.

- [15] Vishay 12CWQ10FNPbF Schottky Rectifier. 2 x 6 A. [www]. <<http://www.vishay.com/docs/94135/94135.pdf>>. Revision: 13-Aug-08
- [16] Bill Roehr & Bryce Shiner. (2001). AN569/D Transient Thermal Resistance - General Data and Its Use. [www]. <http://www.onsemi.com/pub_link/Collateral/AN569-D.PDF>. November. 2001 – Rev. 1.
- [17] CSM3637 current sense resistor. Bulk Metal® Technology High Precision. Current Sensing. Power Surface Mount. Metal Strip Resistor with Resistance Value from 2 mΩ. Rated Power up to 3 W and TCR to 0 ± 15 ppm/°C. [www]. <<http://www.vishay.com/docs/63089/csm.pdf>>. Revision: 13-Jan-09
- [18] AD8210 Analog Device datasheet. High Voltage. Bidirectional Current Shunt Monitor. [www]. <http://www.analog.com/static/imported-files/data_sheets/AD8210.pdf>. Rev A. 04/2007
- [19] NYC0102BLT1G ON Semiconductor datasheet. Sensitive Gate Silicon Controlled Rectifiers. [www]. <http://www.onsemi.com/pub_link/Collateral/NYC0102BL-D.PDF>. December. 2008 – Rev. 0
- [20] IPB081N06L3 G Infineon datasheet. Infineon OptiMOS 3 Power-Transistor. [www]. <http://www.infineon.com/dgdl/IPP_B084N06L3_Rev2.21.pdf?folderId=db3a304313b8b5a60113cee8763b02d7&fileId=db3a30431b3e89eb011b4592273f7db2>. Rev. 2.21
- [21] IR2181 International Rectifier datasheet. IR2181(4)(S) & (PbF) HIGH AND LOW SIDE DRIVER. [www]. <<http://www.irf.com/product-info/datasheets/data/ir2181.pdf>>. Data Sheet No. PD60172 Rev.G
- [22] TLE6250 Infineon datasheet. TLE6250 High Speed CAN-Transceiver. [www]. <[http://www.infineon.com/dgdl/TLE6250G_DS_rev40_Green\[1\].pdf?folderId=db3a30431ed1d7b2011edad13813703&fileId=db3a30431ed1d7b2011edadbb20d3704](http://www.infineon.com/dgdl/TLE6250G_DS_rev40_Green[1].pdf?folderId=db3a30431ed1d7b2011edad13813703&fileId=db3a30431ed1d7b2011edadbb20d3704)> Rev. 4.0. April 2008
- [23] TJA1040T Philips datasheet. TJA1040 High speed CAN transceiver. [www]. <http://www.nxp.com/acrobat_download/datasheets/TJA1040_6.pdf>. 2003 Oct 14
- [24] TJA1040 application note. AN10211 TJA1040 high speed CAN transceiver. [www]. <http://www.nxp.com/acrobat_download/applicationnotes/AN10211_2.pdf>. Rev. 02 – 10 November 2006
- [25] MAX6675 MAXIM datasheet. Cold-Junction-Compensated K-Thermocouple to Digital Converter (0°C to +1024°C). [www]. <<http://datasheets.maxim-ic.com/en/ds/MAX6675.pdf>>. 19-2235; Rev 1; 3/02
- [26] AD595 Analog Device datasheet. Monolithic Thermocouple Amplifiers Cold Junction Compensation. <http://www.analog.com/static/imported-files/data_sheets/AD594_595.pdf>. [www]. Rev.C.
- [27] TLC274 Texas Instruments datasheet. TLC274. TLC274A. TLC274B. TLC274Y. TLC279 LinCMOS PRECISION QUAD OPERATIONAL AMPLIFIERS. [www]. <<http://focus.ti.com/lit/ds/symlink/tlc274.pdf>>. September 1987 – Revised March 2001
- [28] Wärtsilä 34SG Engine Technology for compressor drive. [www]. <http://www.wartsila.com/Wartsila/global/docs/en/power/media_publications/brochures/wartsila34SGengine-technology-for-compressor-drives-2008.pdf>.

- [29] HCPL-0600 Fairchild Semiconductors datasheet. *High Speed-10 MBit/s Logic gate Optocouplers*. [www]. <<http://www.fairchildsemi.com/ds/HC/HCPL-0600.pdf>>. 1/7/04
- [30] LM258 National Semiconductors datasheet. *LM158/LM258/LM358/LM2904 Low Power Dual Operational Amplifiers*. [www]. <<http://www.national.com/ds/LM/LM258.pdf>>. October 2005
- [31] LM2901 National Semiconductors datasheet. *LM139/LM239/LM339/LM2901/LM3302 Low Power Low Offset Voltage Quad Comparators*. [www]. <<http://www.national.com/ds/LM/LM2901.pdf>>. March 2004
- [32] *Sharp PC357N Series Mini-flat Package, General Purpose Photocoupler*. [www]. <http://document.sharpsma.com/files/pc357n_eJ.pdf>. Sheet No.: D2-A00101EN
Date Sep. 30. 2003.
- [33] Schmitt trigger 74HC14 datasheet. *74HC14; 74HCT14 Hex inverting Schmitt trigger*. [www]. <http://www.nxp.com/acrobat_download/datasheets/74HC_HCT14_3.pdf>. 2003 Oct 30.
- [34] OPA551 Texas Instruments datasheet. *High Voltage. High Current Operational Amplifier*. [www]. <<http://focus.ti.com/lit/ds/symlink/opa551.pdf>>. SBOS100A – July 1999 – Revised October 2003
- [35] EL2001C Intersil datasheet. *EL2001C Low Power. 70 MHz Buffer Amplifier*. [www]. <http://www.datasheetcatalog.com/datasheets_pdf/E/L/2/0/EL2001C.shtml>. December 1995 Rev G.
- [36] OP491 Analog Device datasheet. *Micropower Single-Supply Rail-to-Rail Input/Output Op Amps OP191/OP291/OP491*. [www]. <http://www.analog.com/static/imported-files/data_sheets/OP191_291_491.pdf>. Rev. D.
- [37] Voltage regulator. *MC78L00A Series. NCV78L00A 100 mA Positive Voltage Regulators*. [www]. <http://www.onsemi.com/pub_link/Collateral/MC78L00A-D.PDF>. September. 2007 - Rev. 13.
- [38] AD8608 Analog Device datasheet. *Precision. Low Noise. CMOS. Rail-to-Rail. Input/Output Operational Amplifiers AD8605/AD8606/AD8608*. [www]. <http://www.analog.com/static/imported-files/data_sheets/AD8605_8606_8608.pdf>. Rev. I.
- [39] LM2576 National Semiconductor datasheet. *LM2576/LM2576HV Series SIMPLE SWITCHER® 3A Step-Down Voltage Regulator*. [www]. <<http://www.national.com/ds/LM/LM2576.pdf>>. August 2004
- [40] LP3962 National Semiconductor datasheet. *LP3962/LP3965 1.5A Fast Ultra Low Dropout Linear Regulators*. [www]. <<http://www.national.com/ds/LP/LP3962.pdf>>. September 2006.
- [41] MC7812 ON Semiconductor datasheet. *MC7800. MC7800A. MC7800AE. NCV7800 1.0 A Positive Voltage Regulators*. [www]. <http://www.onsemi.com/pub_link/Collateral/MC7800-D.PDF>. March. 2008 - Rev. 18
- [42] LM2576 ON Semiconductor datasheet. *LM2576 3.0 A. 15 V. Step-Down Switching Regulator*. [www]. <http://www.onsemi.com/pub_link/Collateral/LM2576-D.PDF>. January. 2006 – Rev. 8.

- [43] PCB isolation rules. Elmatica AS.
<<http://www.elmatica.no/website.aspx?displayid=1188>>
- [44] ELFA Factsheet. *Factsheet*. [www].
<https://www1.elfa.se/data1/wwwroot/webroot/Z_STATIC/en/pdf/fakta55.pdf>
- [45] Keystone spacers and standoffs. *Swage/Force Fit Standoffs*. [www].
<<http://www.keyelco.com/pdfs/M55p65.pdf>>
- [46] Phoenix Contact ZFKDS 2,5-5,08. *ZFKDS 2,5-5,08*. [www].
<<http://eshop.phoenixcontact.se/phoenix/treeViewClick.do?UID=2900173&general=s es>>.
- [47] *MIL-HDBK-217F MILITARY HANDBOOK RELIABILITY PREDICTION OF ELECTRONIC EQUIPMENT*. [www]. <<http://www.sqconline.com/download/MIL-HDBK-217F.pdf>>. MIL-HDBK-217F 2 December 1991.
- [48] *MIL-HDBK-217F Notice 2 MILITARY HANDBOOK RELIABILITY PREDICTION OF ELECTRONIC EQUIPMENT*. [www]. <<http://www.sqconline.com/download/MIL-HDBK-217F-CHANGE-NOTICE-2.pdf>>. NOTICE 2 28 February 1995.

Appendix 1 shows the top layer, mid layer 1, internal plane 1, bottom layer, top silkscreen and bottom silkscreen of the cylinder module PCB.

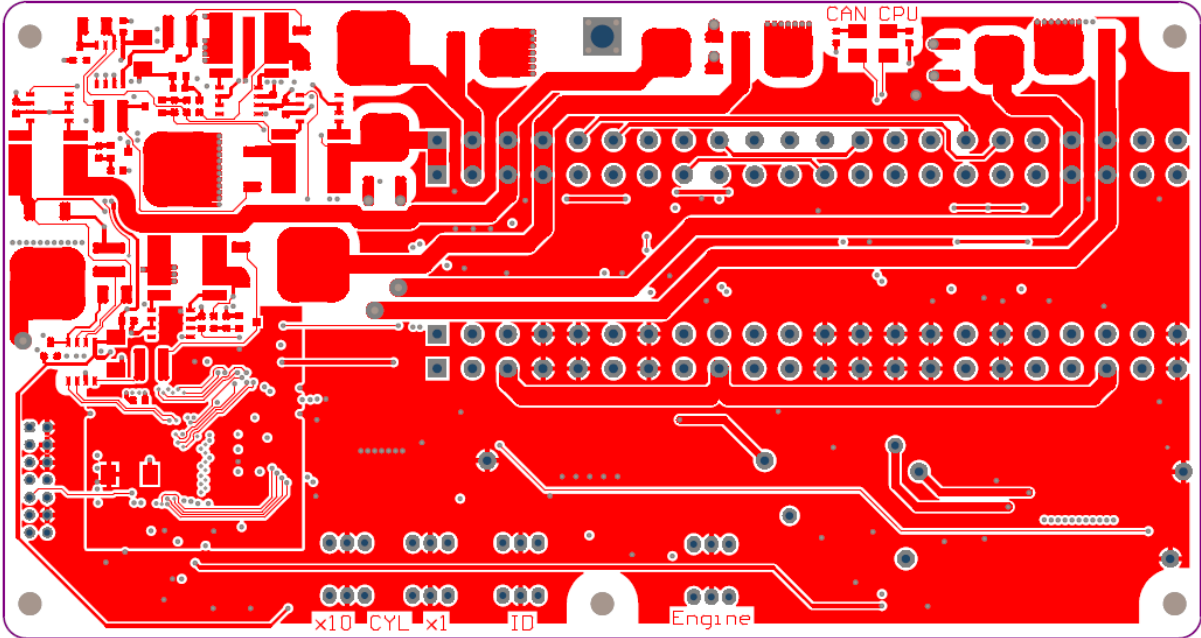


Figure 1: CM Top layer

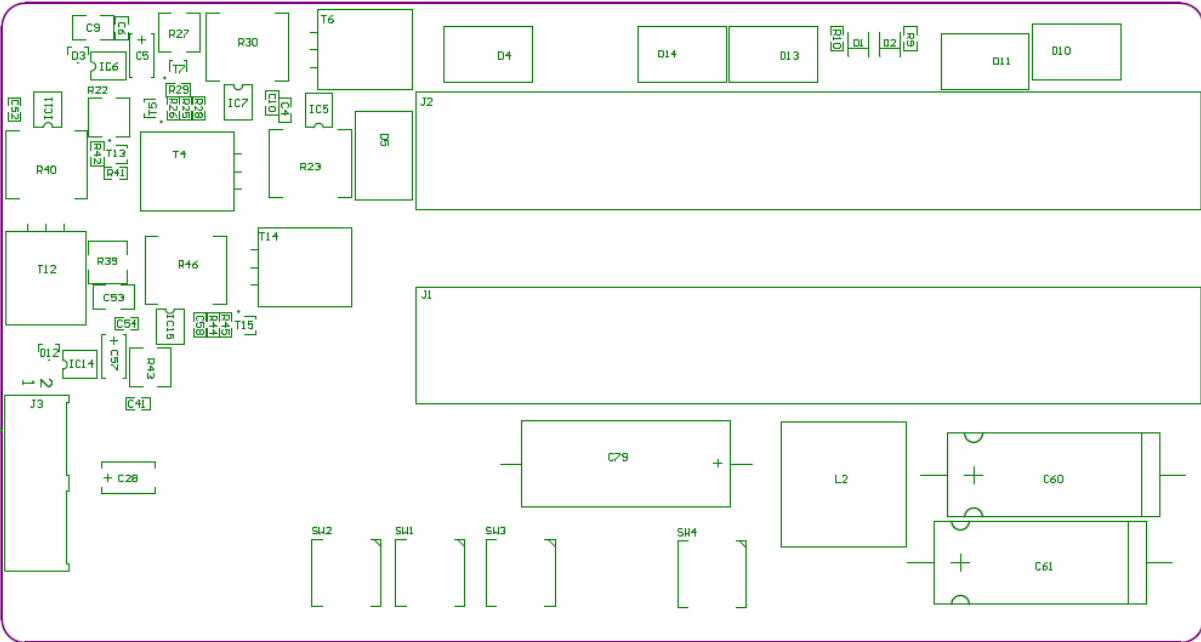


Figure 2: CM Top silkscreen

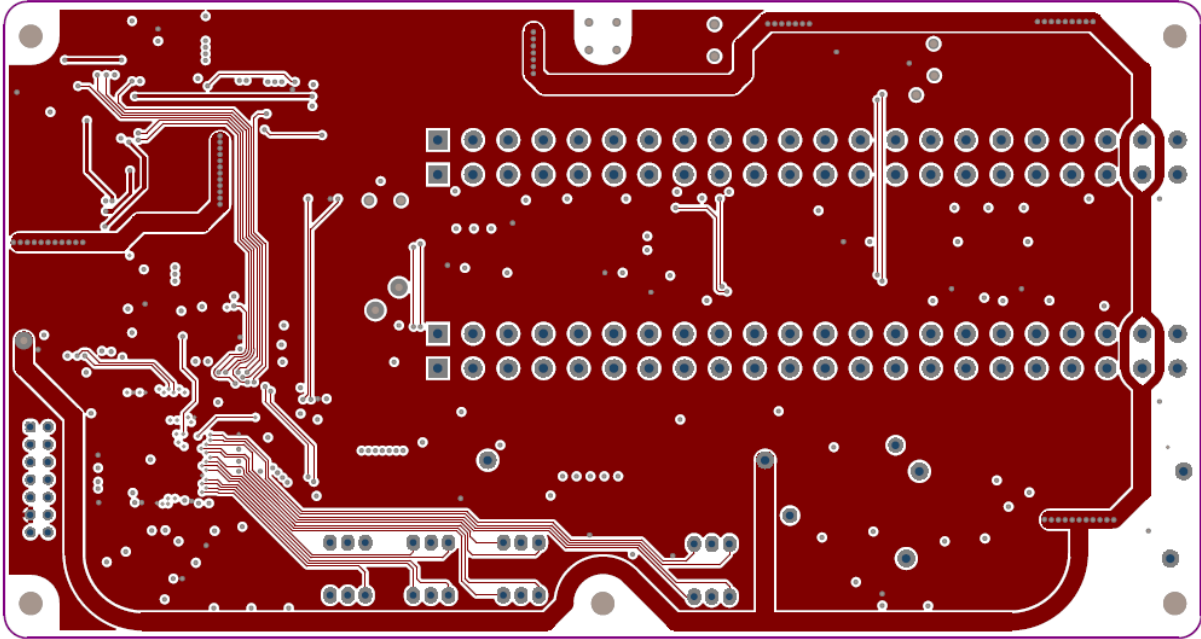


Figure 3: CM Midlayer1

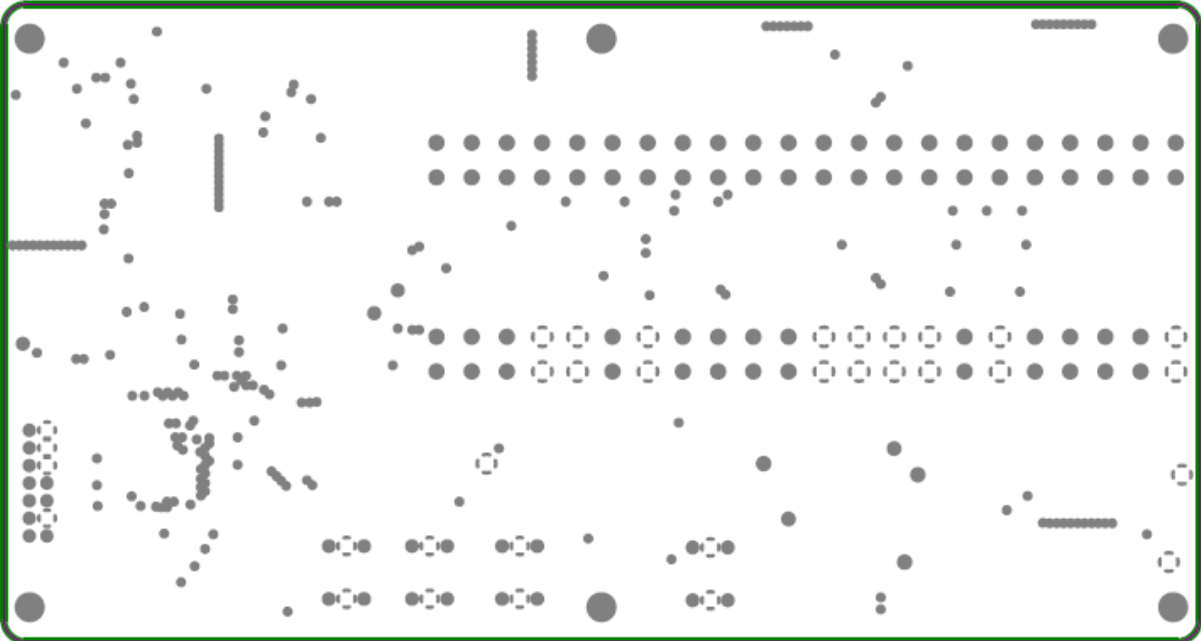


Figure 4: CM Internal plane1 (GND). Inverted drawing (white is the plane, green is no copper and grey circles are pads and vias not connected to the plane. Pads connected to the plane are shown as 4 grey areas around a white pad).

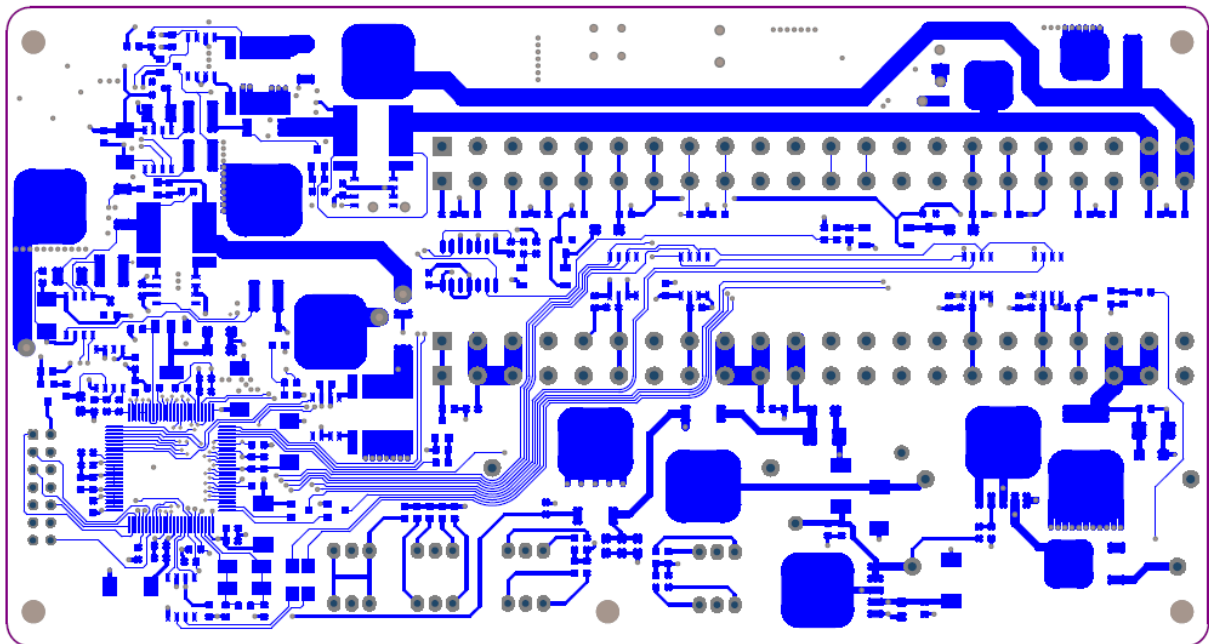


Figure 5: CM Bottom layer (not mirrored - as seen in the PCB layout program)

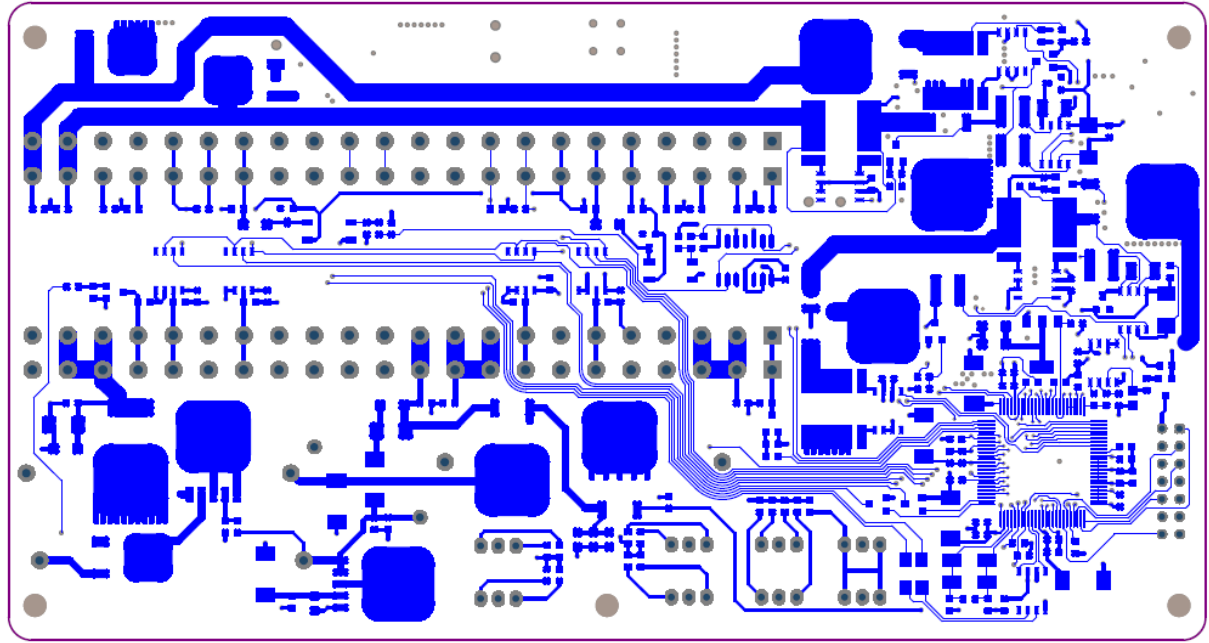


Figure 6: CM Bottom layer (mirrored – as seen on the PCB)

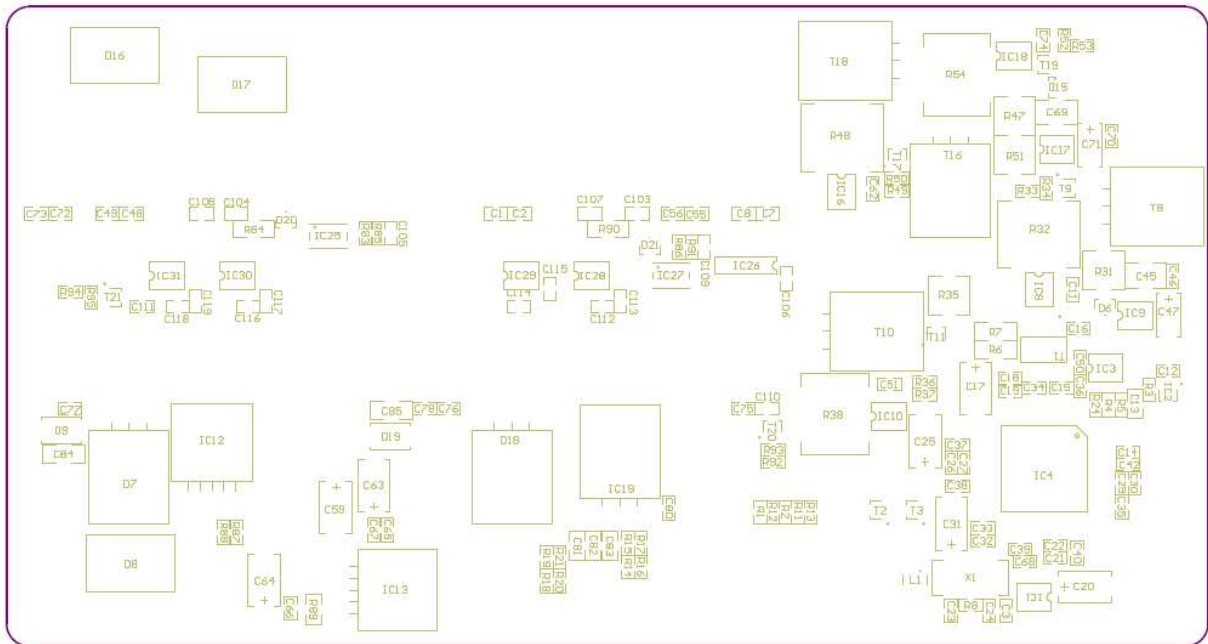


Figure 7: CM Bottom silkscreen (mirrored – as seen on the PCB)

Appendix 2 shows the top layer, internal plane 1, internal plane 2, bottom layer, top silkscreen and bottom silkscreen of the knock module PCB.

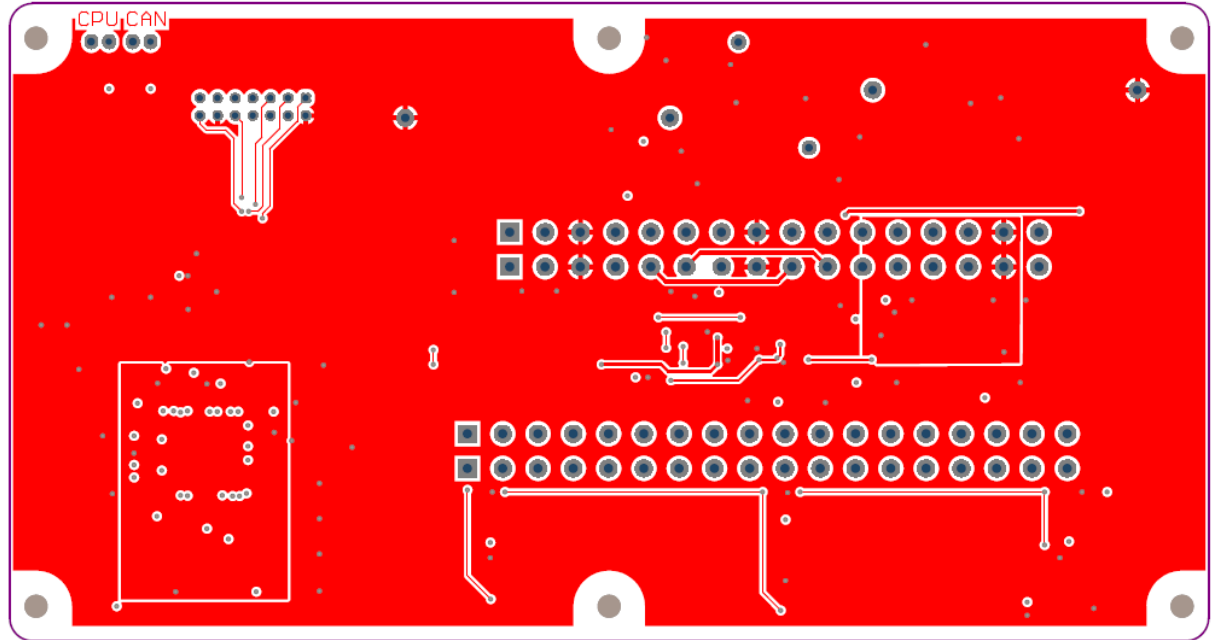


Figure 1: KM Top layer

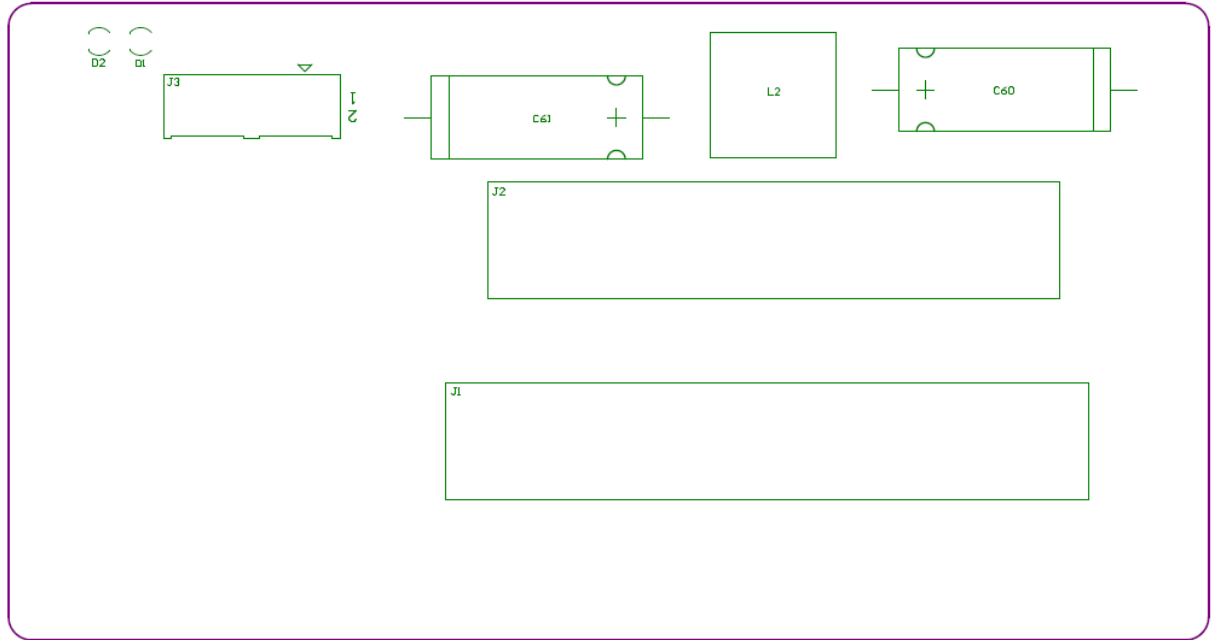


Figure 2: KM Top silkscreen

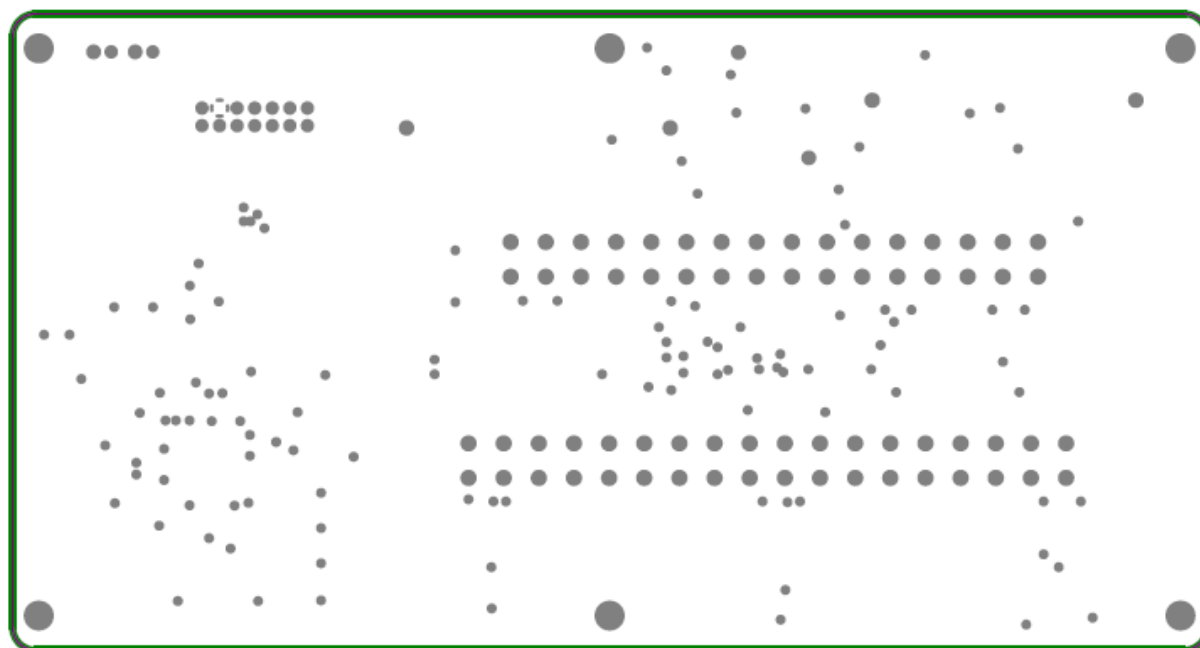


Figure 3: KM Internal plane1 (VCC). Inverted drawing (white is the plane, green is no copper and grey circles are pads and vias not connected to the plane. Pads connected to the plane are shown as 4 grey areas around a white pad).

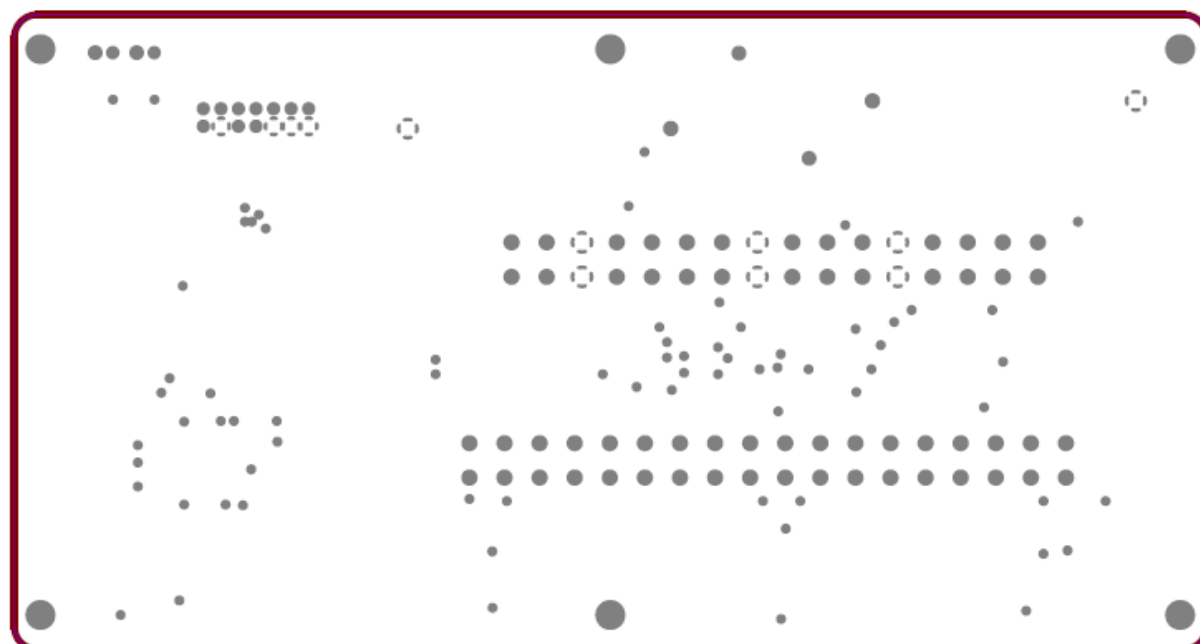


Figure 4: KM Internal plane2 (GND). Inverted drawing (white is the plane, brown is no copper and grey circles are pads and vias not connected to the plane. Pads connected to the plane are shown as 4 grey areas around a white pad).

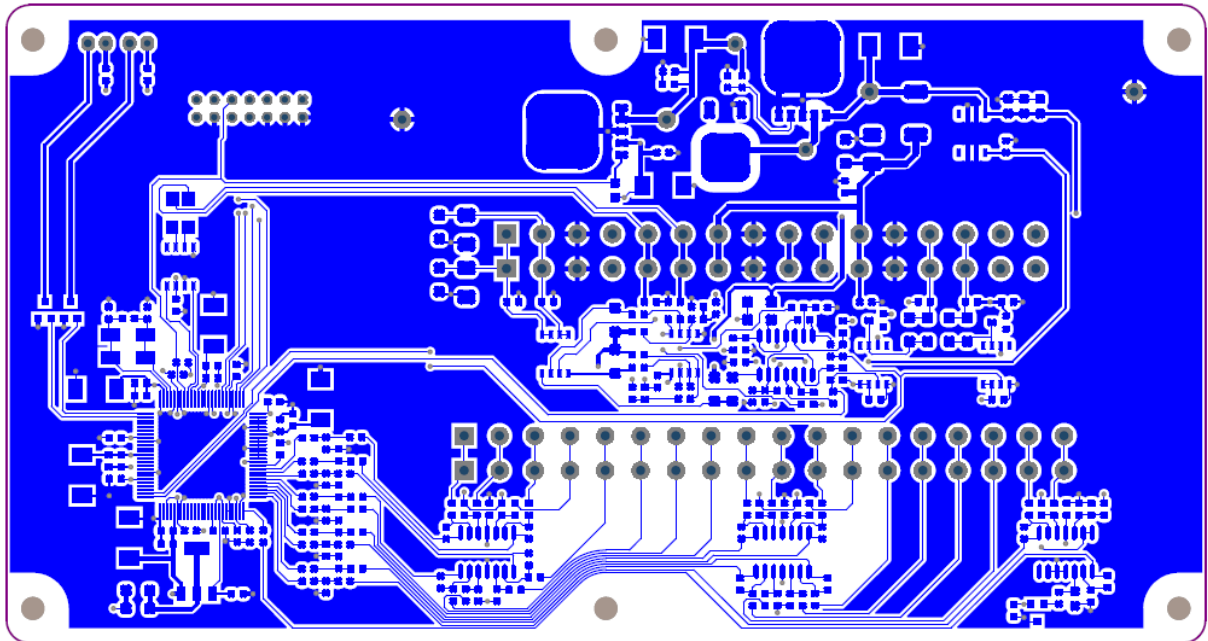


Figure 5: KM Bottom layer (not mirrored - as seen in the PCB layout program)

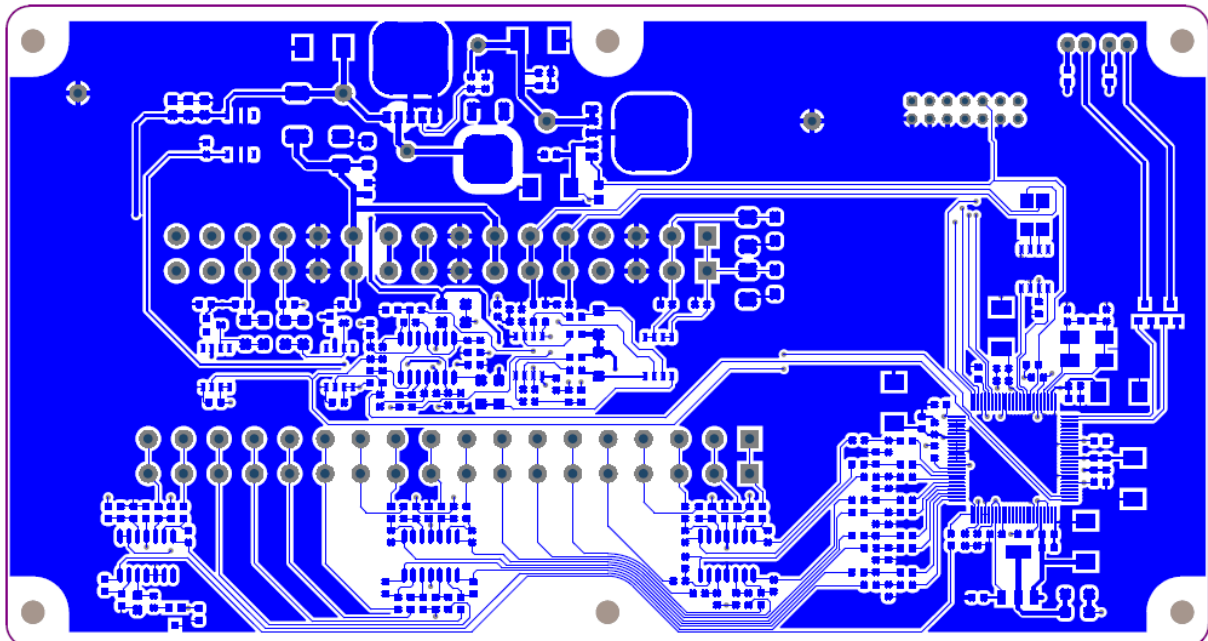


Figure 6: KM Bottom layer (mirrored – as seen on the PCB)

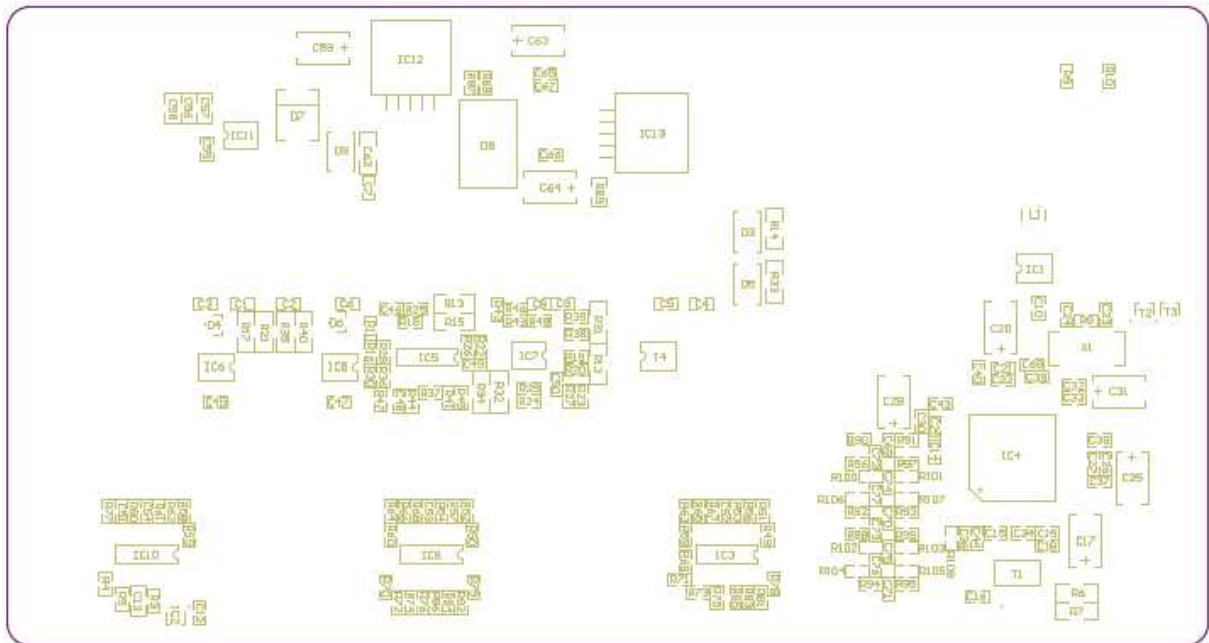


Figure 7: CM Bottom silkscreen (mirrored – as seen on the PCB)

Topic:	Customer Requirements Document	
Summary:	This document defines the high level requirements for the face lift of EMS. The priority of the requirements are given (1: High importance, 2: Desired)	
Highlights:		

Table of Contents

1	BACKGROUND	2
2	TOP LEVEL REQUIREMENTS, SUMMARY	3
3	TOP LEVEL REQUIREMENTS, DETAILS	4
4	TEST PLAN FOR CUSOMER REQUIREMENTS	7
5	DOCUMENT INFORMATION	8



1 Background

The idea with this work is to make a face lift of the EMS design from 1994. There are more than 600 engines with EMS and the majority of them will be in operation beyond 2020. The face lift will guarantee spare parts of the Cylinder Module (CM) and Knock Module (KM) for at least the next 15 years. This project will inquire the possibility of a design with only one board for the CM and one board for the KM or one and the same board for both CM and KM. Today the CM and the KM have one CPU board and one I/O board. The CPU board is the same for both CM and KM but the I/O boards are different.

The mechanical design of the casing and functionality of the system must not change. To guarantee a long life time some components must be changed with state of the art components.

1.1 EMS Face Lift

Requirements:

- 1. Functional equivalence with current EMS**
- 2. Fit within the same casing as the current system**
- 3. Guarantee long life time of the system**
- 4. 36000 h operating time**

Objectives:

- 1. Replace the CPU and I/O boards with one board for CM and one for KM**
- 2. Replace the CPU and I/O boards with one board for both CM and KM**
- 3. Increase the mechanical reliability of the system**
- 4. Decrease the number of different hardware versions**

2 Top level requirements, summary

This section summarizes the top level customer requirements for the face lift of EMS.

The requirements are categorised the following way

- 1: High importance means that the requirement must be fulfilled within this project.
- 2: Desirable means that we shall plan to implement and test for this requirement as it has a customer value but we are allowed to skip the final implementation / testing or reporting of this requirement if we cannot meet this requirement.
- 3: Not included means that this is not a requirement for this project.

REQ ID	Title	Short description / Purpose	Category 1: High importance 2: Desirable 3: Not included	Derived from
CREQ-1	Functional equivalence with current EMS	The face lift of EMS cannot change any functions of the system.	1	Req. 1
CREQ-2	Fit within the same casing as the current system	The same casing has to be used as for the system of today.	1	Req. 2
CREQ-3	Guarantee long life time of the system	Design with current state of the art components to guarantee long life time of the system.	1	Req. 3
CREQ-4	36000 h operating time	It is recommended by the customer to replace the system after 36000 h	1	Req. 4
CREQ-5	Replace the CPU and I/O boards with one board for CM and one for KM	The production is cheaper and easier if one board is used instead of one CPU board and one I/O board in each CM and KM.	2	Obj. 1
CREQ-6	Replace the CPU and I/O boards with one board for both CM and KM	Use the same board for CM and KM. Mount different components on the board for CM and KM.	2	Obj. 2
CREQ-7	Increase the mechanical reliability of the system	Design without flat conductor cable, screwed contact and power components screwed to the case.	2	Obj. 3
CREQ-8	Decrease the number of different hardware versions	The production is easier if less hardware version is used.	2	Obj. 4
CREQ-9	Investigate the possibility of replacing the MC	The MC is no longer in production. Replace the MC if it is easy.	2	Obj. 5

3 Top level requirements, details

3.1 Overview

Each requirement is documented using the template shown below.

Requirement number	Requirement name	Originates / Requested by	Priority
A unique number used for requirement traceability	The name of the requirement	Where does the requirement originate from or who requested this requirement	1: High importance 2: Desirable 3. Not included in this project phase
Description			
A short textual description of the requirement			
Validation			
A short textual description of how the requirement shall be validated			
References/Discussion/Implementation			
References to other documents. Notes from discussions and implementation proposals.			

3.2 Top level Requirement details

Requirement number	Requirement name	Originates / Requested by	Priority
CREQ-1	Functional equivalence with current EMS	Hoerbiger	1
Description			
The face lift of EMS cannot change any functions, it should just increase the mechanical reliability, life time etc.			
Validation			
Design review, HIL-test and field test.			
References/Discussion/Implementation			
The current test equipment test the CPU and I/O boards separately, therefore must a new test equipment be built.			

Requirement number	Requirement name	Originates / Requested by	Priority
CREQ-2	Fit within the same casing as the current system	Hoerbiger	1
Description			
The face lift of EMS will only change the circuit boards, components and software. On the outside it will look exactly the same.			
Validation			
Mounting the board in the same CM/KM case.			
References/Discussion/Implementation			

Requirement number	Requirement name	Originates / Requested by	Priority
CREQ-3	Guarantee long life time of the system	Hoerbiger	1
Description			
Use current state of the art components to guarantee a long life of the system			
Validation			
Design review and environmental tests.			
References/Discussion/Implementation			

Requirement number	Requirement name	Originates / Requested by	Priority
CREQ-4	36000 h operating time	Hoerbiger	1
Description			
It is recommended by the customer to replace the system after 36000 h.			
Validation			
MTBF calculations.			
References/Discussion/Implementation			

Requirement number	Requirement name	Originates / Requested by	Priority
CREQ-5	Replace the CPU and I/O boards with one board for CM and one for KM	Hoerbiger	2
Description			
The production is cheaper and easier if one board is used instead of one CPU board and one I/O board in each CM and KM.			
Validation			
References/Discussion/Implementation			

Requirement number	Requirement name	Originates / Requested by	Priority
CREQ-6	Replace the CPU and I/O boards with one board for both CM and KM	Hoerbiger	2
Description			
Replace the CPU and I/O boards with one board for both CM and KM by replacing some hardware with software and choosing small components.			
Validation			
References/Discussion/Implementation			

Requirement number	Requirement name	Originates / Requested by	Priority
CREQ-7	Increase the mechanical reliability of the system	Hoerbiger	2
Description			
Increase the mechanical reliability of the system by choosing reliable components and making a good design with fewer components. Design without flat conductor cable, screwed contact and power components screwed to the case.			
Validation			
Design review and environmental tests.			
References/Discussion/Implementation			

Requirement number	Requirement name	Originates / Requested by	Priority
CREQ-8	Decrease the number of different hardware versions	Hoerbiger	2
Description			
There are different hardware versions for different engines.			
Validation			
Design review.			
References/Discussion/Implementation			

4 Test plan for Customer requirements

4.1 Test plan

The test of the new EMS will be done by design review, HIL-test and field test. The current test equipment test the CPU and I/O boards separately, therefore a new test equipment must be built.

5 Document Information

5.1 Change history

Revision	Author	Date	Reason for Change
Draft 0.1	Ulrika Ahlquist	2009-01-21	Draft for review
Draft 0.2	Ulrika Ahlquist	2009-01-22	Validations updated after review by MGr
Draft 0.3	Ulrika Ahlquist	2009-01-26	Updated after review by AG, BNA, GB and MGr
Issue 1.0	Ulrika Ahlquist	2009-01-26	Approved by MGr

5.2 HOERBIGER Control Systems reference documents

#	Reference	Name

5.3 Customer approval

Revision	Approver	Date	Notes

5.4 Customer reference documents

#	Reference	Name

5.5 External reference documents

#	Reference	Name